HIGH ENERGY EMISSION FROM THE MILLISECOND PULSAR POPULATION IN GLOBULAR CLUSTERS

DAVID C. Y. HUI On behalf of Fermi Asian Network

DEPARTMENT OF ASTRONOMY & SPACE SCIENCE
CHUNGNAM NATIONAL UNIVERSITY
SOUTH KOREA

The extreme Universe viewed in very-high-energy gamma-ray 2021
22 February 2022

1. MSPs in the Galactic field (GF)
2. Dynamical formation of MSPs in globular clusters (GCs)
3. Comparative analysis: GC MSPs vs. GF MSPs
4. Current status and future prospects of gamma-ray observations of GC MSP populations

MILLISECOND PULSAR (MSP)

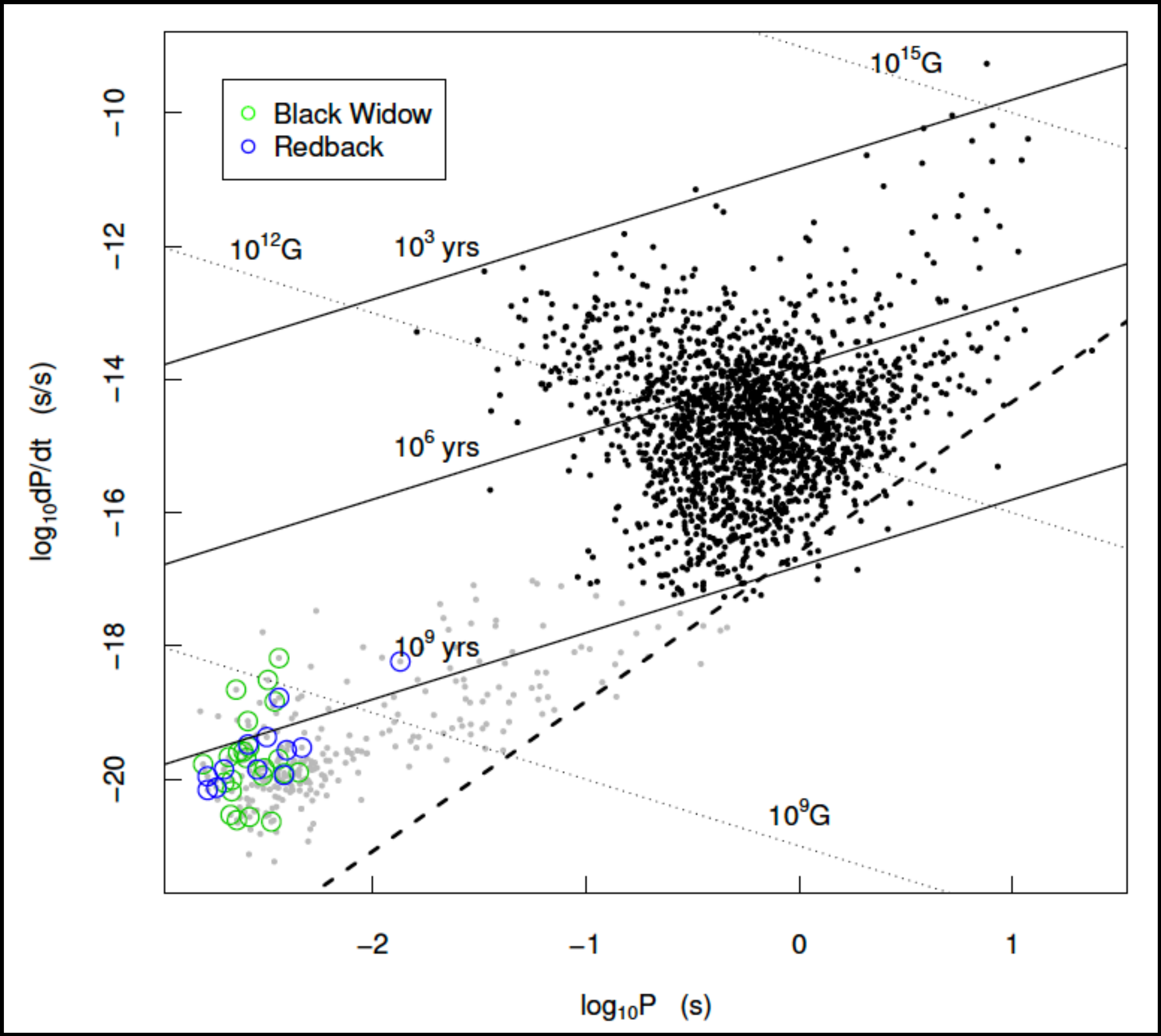

Hui & Li (2019)

MILLISECOND PULSAR (MSP)

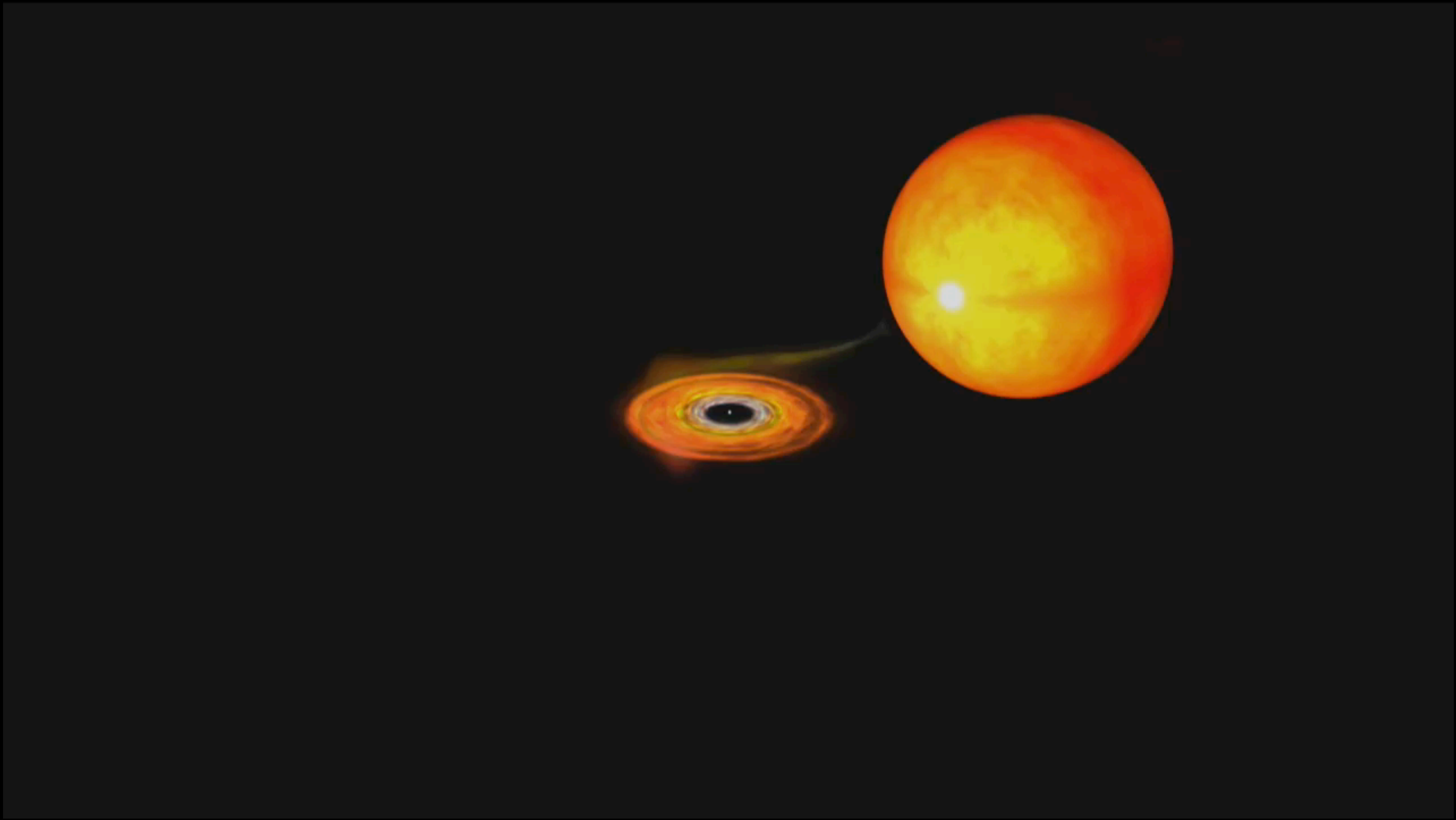

Animation courtesy: CXC

MILLISECOND PULSAR (MSP)

Various channels for MSP formation

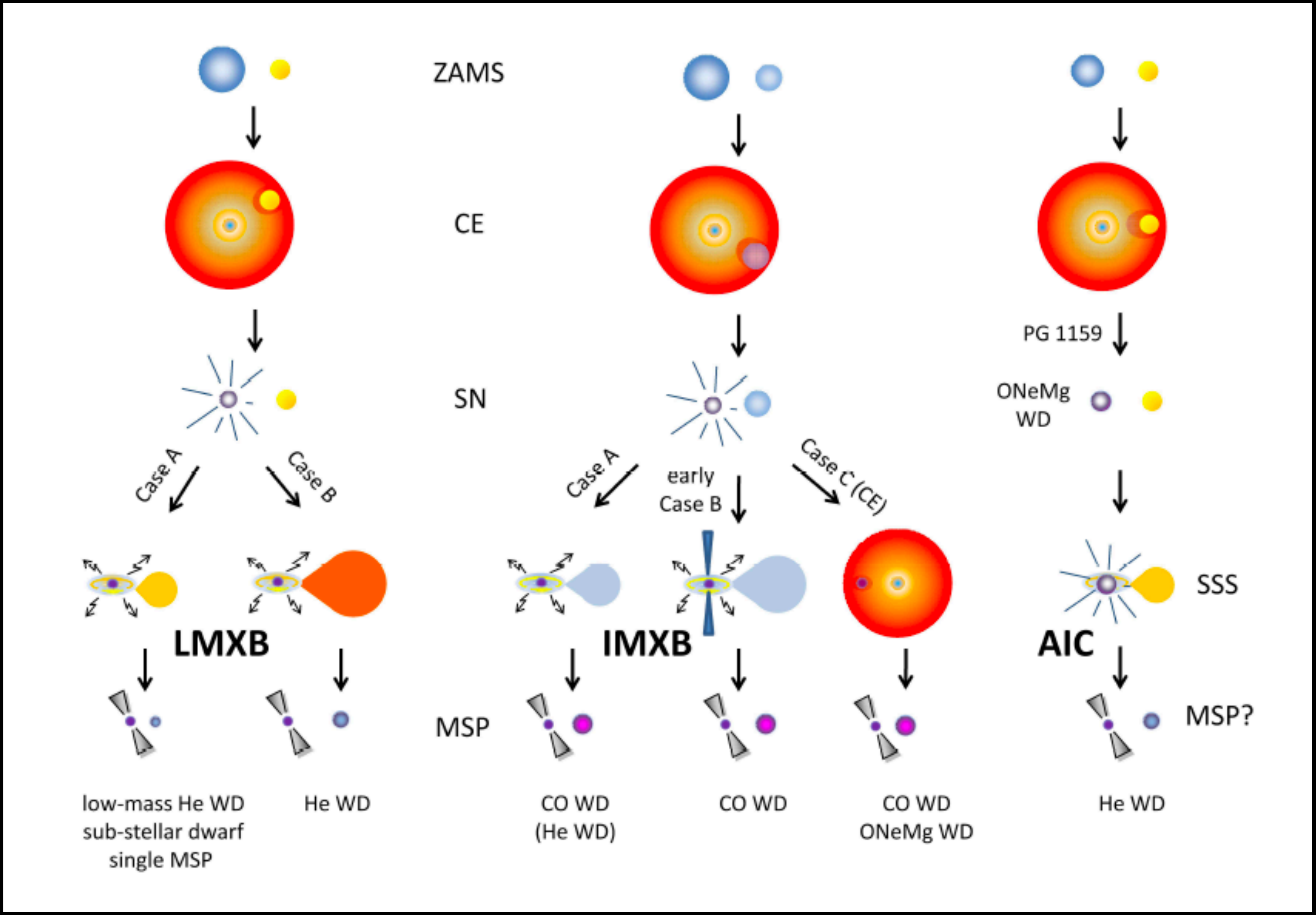

Tauris 2011

MSP ZOO

- Black Widow $M_2 \sim 0.02 - 0.05 M_\odot$
- Tidarren $M_2 < 0.015 M_\odot$
- Redback $M_2 \sim 0.2 - 0.4 M_\odot$

} Spider MSPs $P_b < 1$ day

- MSP-Planet system
- Isolated MSP
- Wide-orbit MSP binary (with He/CO WD companions)

BLACK WIDOWS

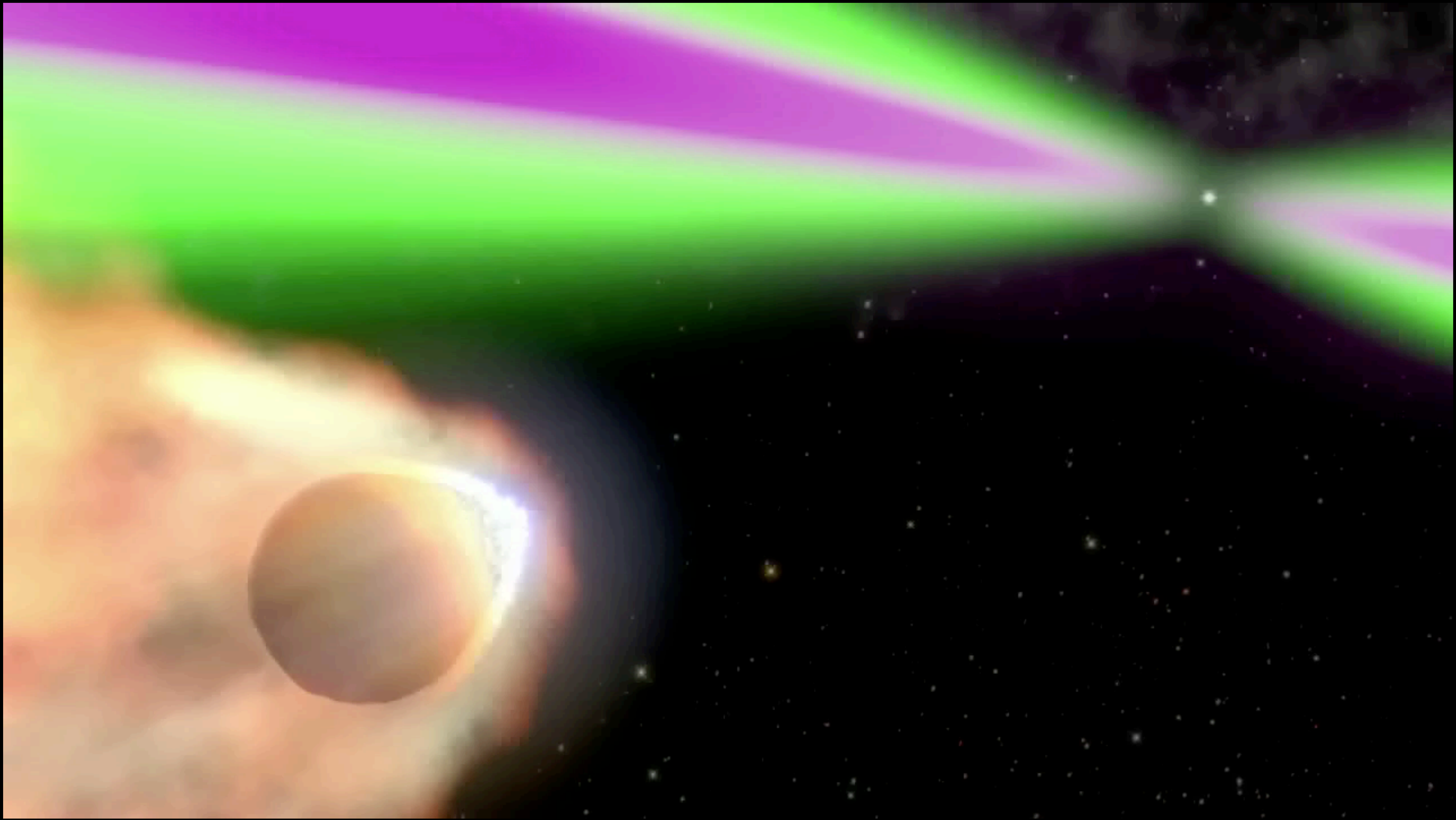

Animation courtesy: CXC

REDBACKS

Swinging between rotation-power state and accretion-power state

Animation courtesy: CXC

X-RAY PROPERTIES OF GF MSP

Bright and hard X-ray emission from RBs can be accounted by the prominent contribution from the intrabinary shocks.

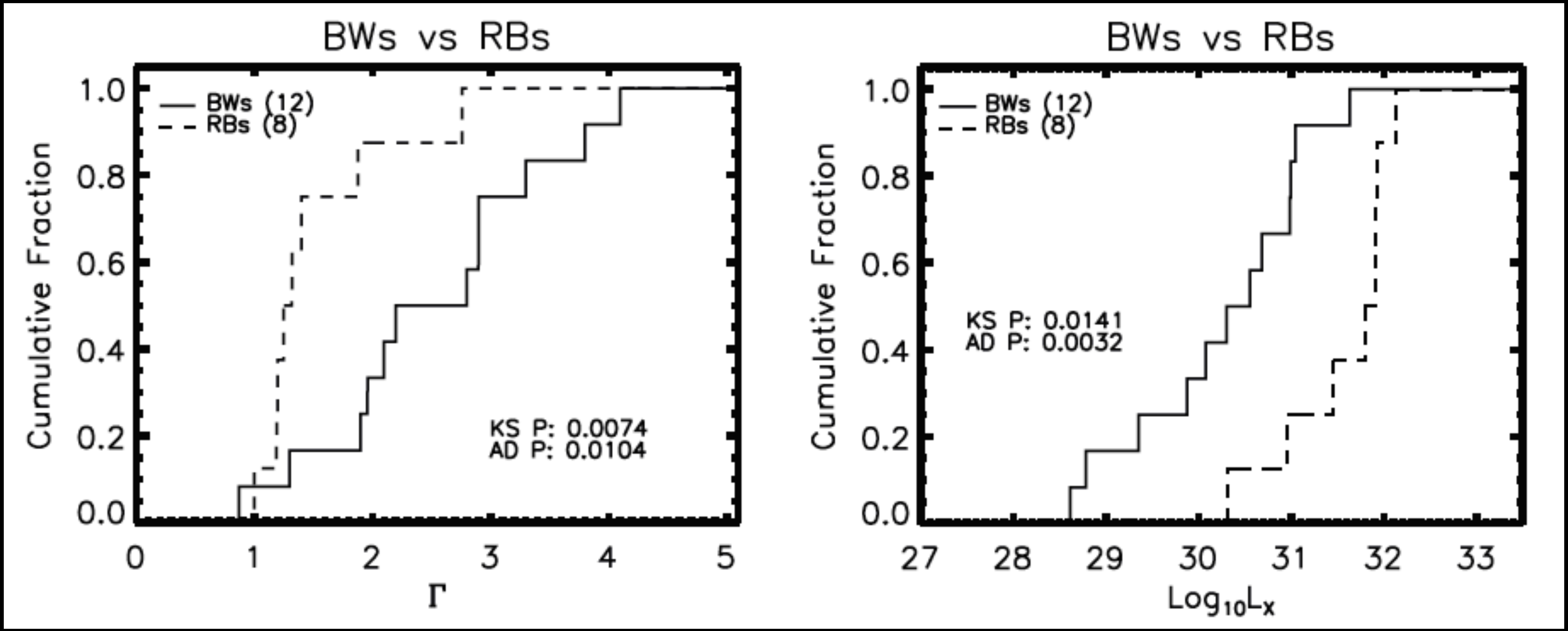

Lee et al. (2018)

X-RAY PROPERTIES OF GF MSP

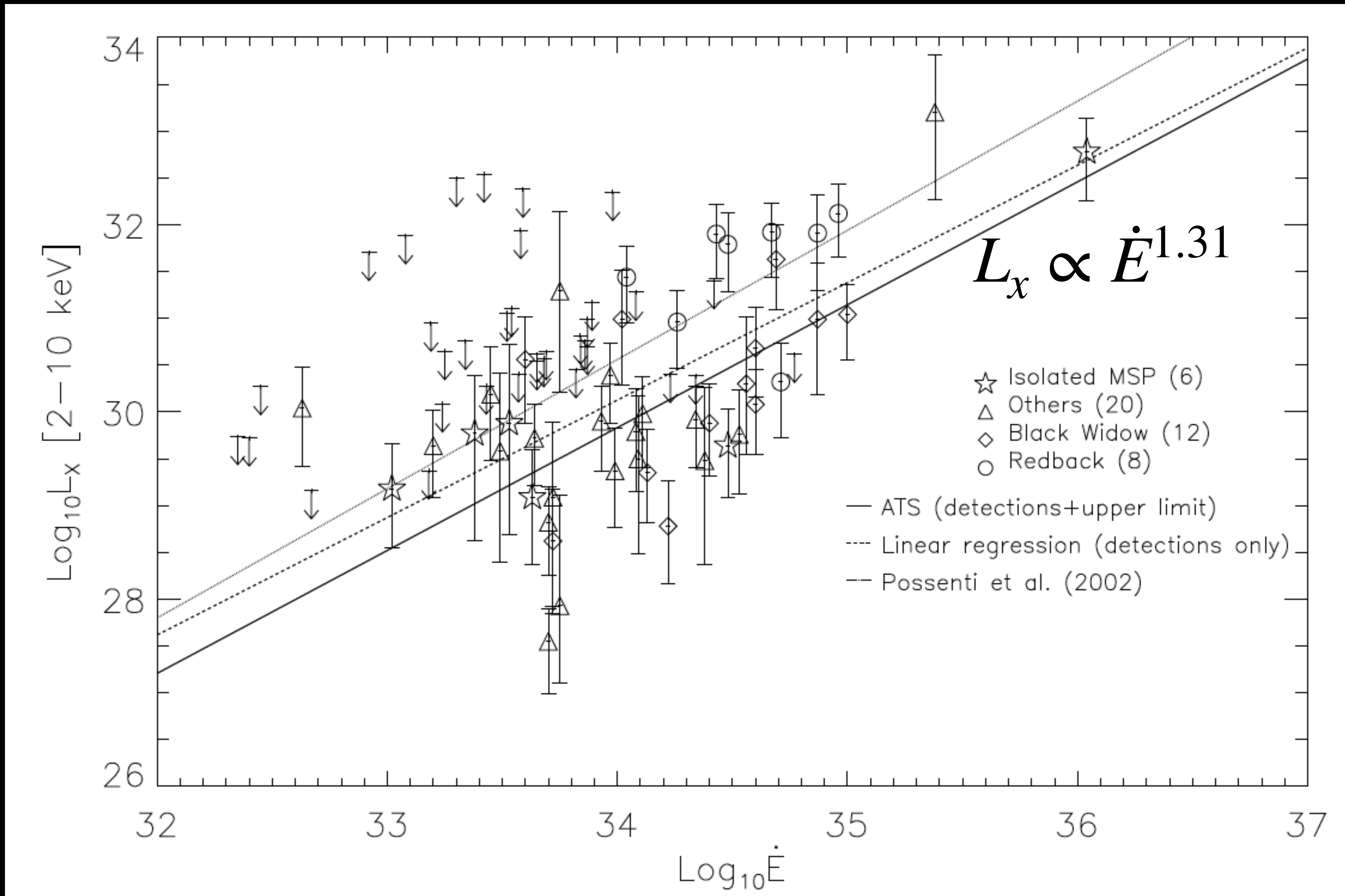

Lee et al. (2018)

GAMMA-RAY PROPERTIES OF GF MSP

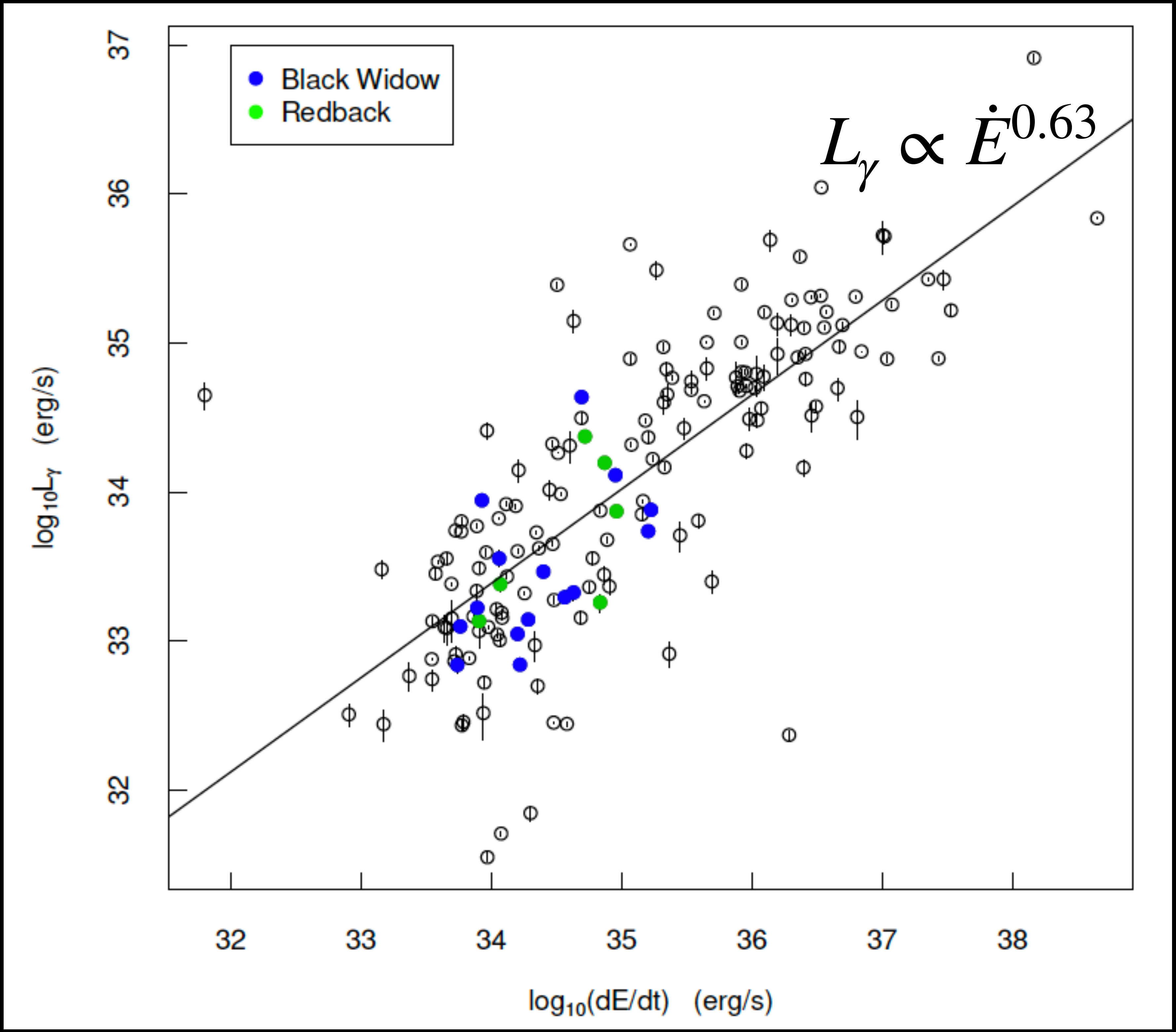

Hui & Li (2019)

GAMMA-RAY PROPERTIES OF GF MSP

No significant difference in the gamma-ray properties between RBs and BWs

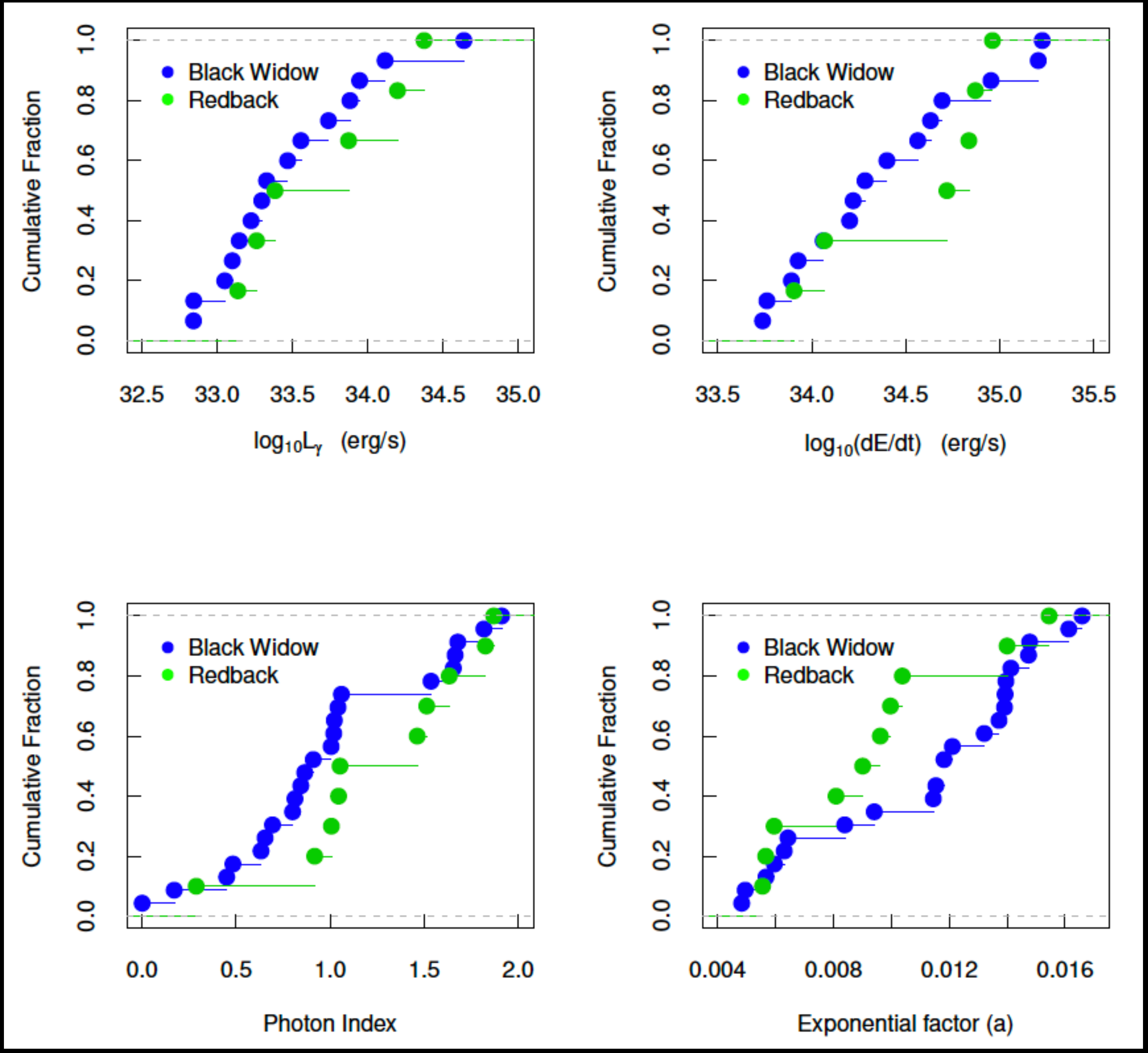

Hui & Li (2019)

GLOBULAR CLUSTER (GC)

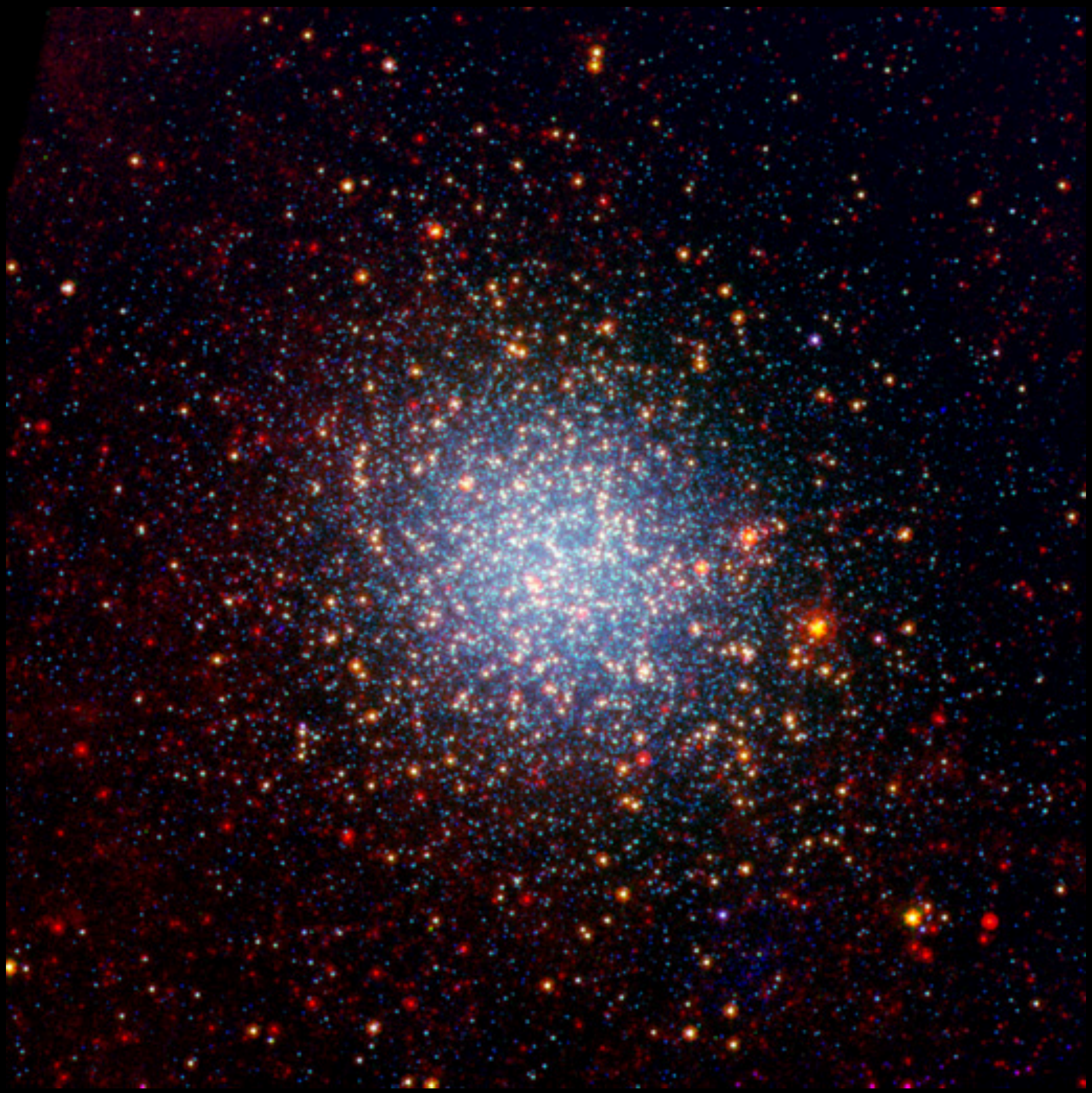

- Stellar systems tightly bounded by gravity
- Mainly consist of late-type stars
- Stellar density increases towards center
- Frequent stellar encounter in the core

STELLAR ENCOUNTER IN GC

Credit: A. M. Geller

DYNAMICAL FORMATION OF COMPACT BINARIES

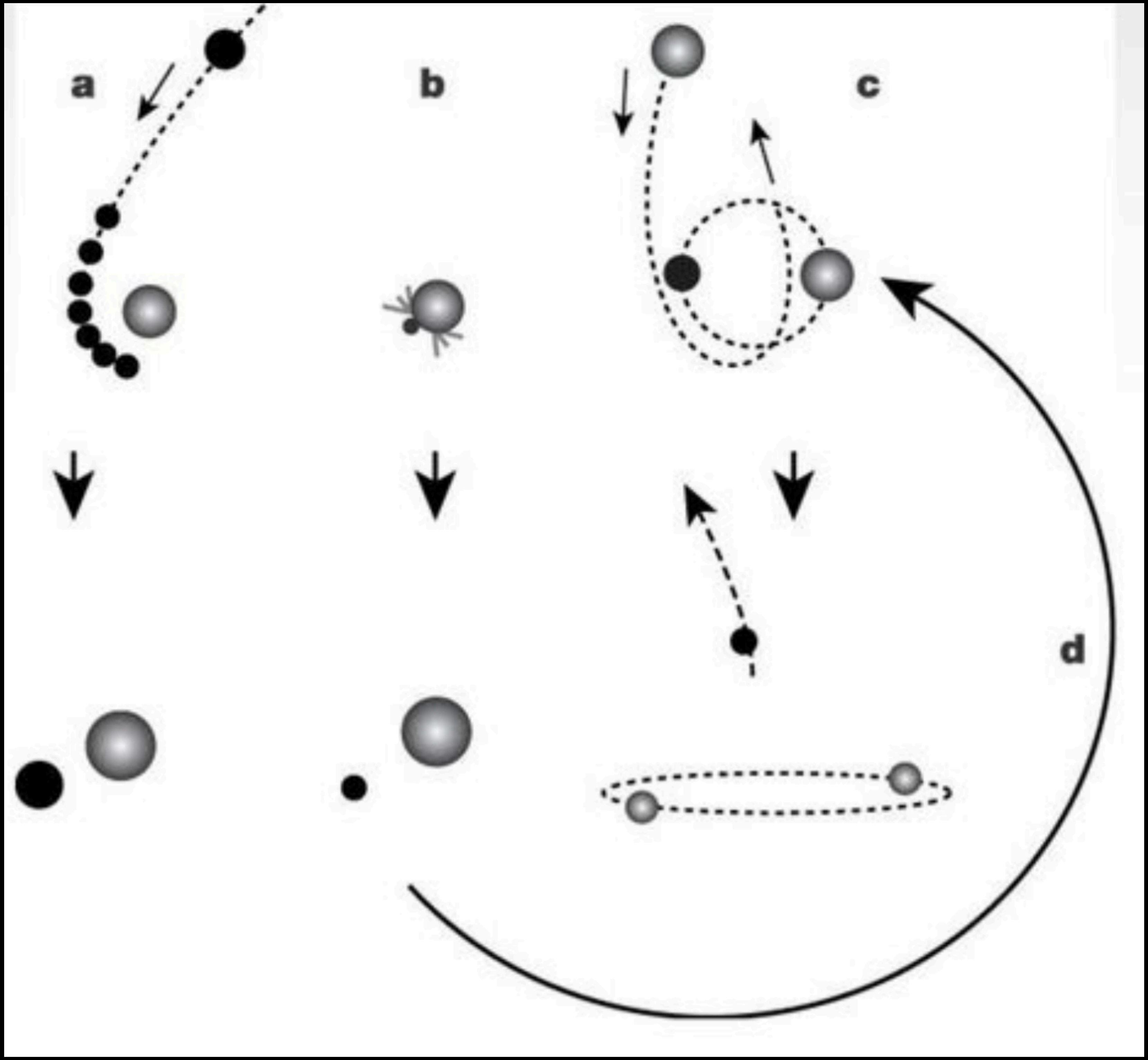

DYNAMICAL FORMATION OF GC MSP

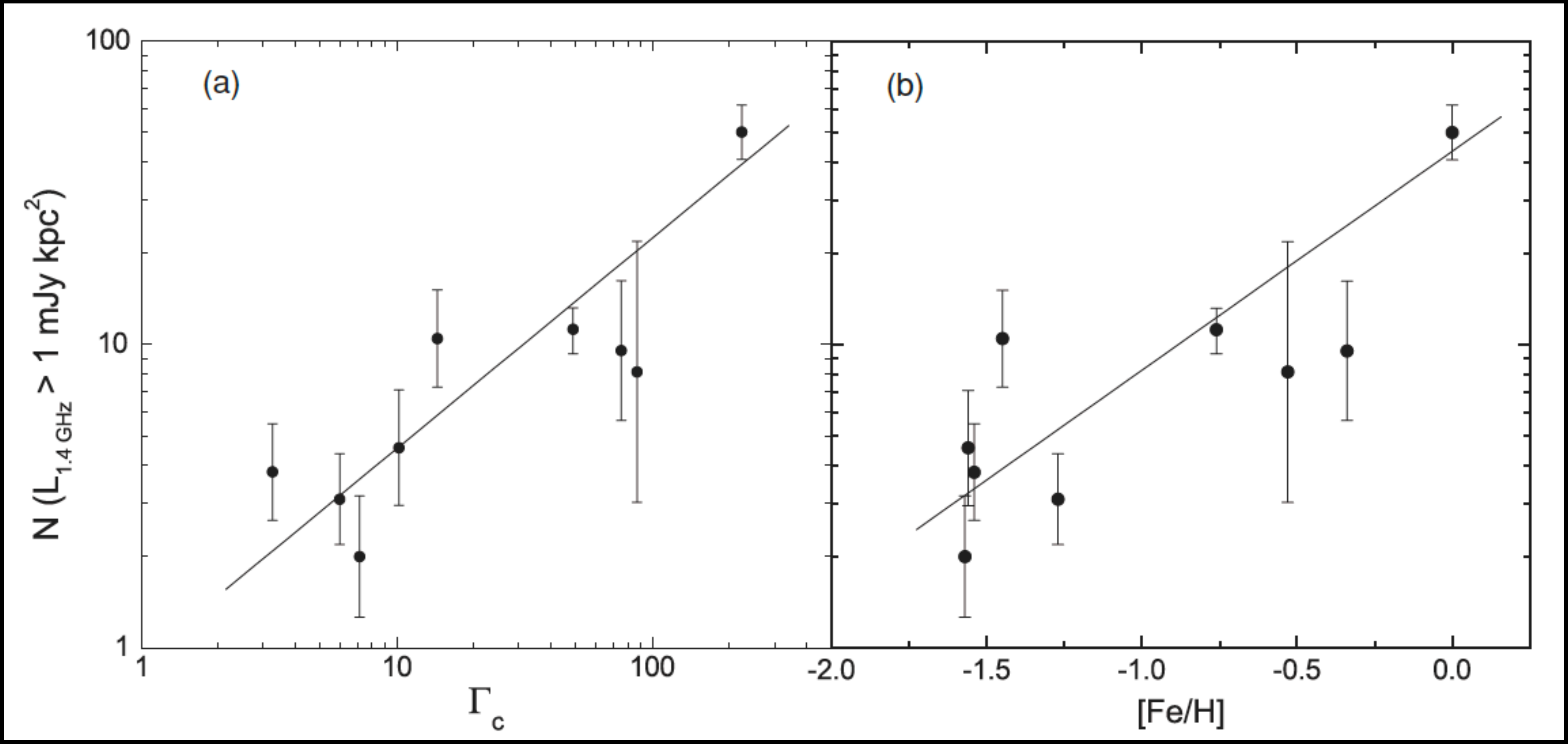

Hui, Cheng & Team (2010)

DYNAMICAL FORMATION OF COMPACT BINARIES

- Frequent stellar encounters make GCs as MSP factories
- In comparison with GF MSPs, the evolution of MSPs/their progenitors in GCs can be altered by such encounters
- Dynamical interaction can leave imprints on their physical properties (e.g. rotation, B-field, X-ray nature)

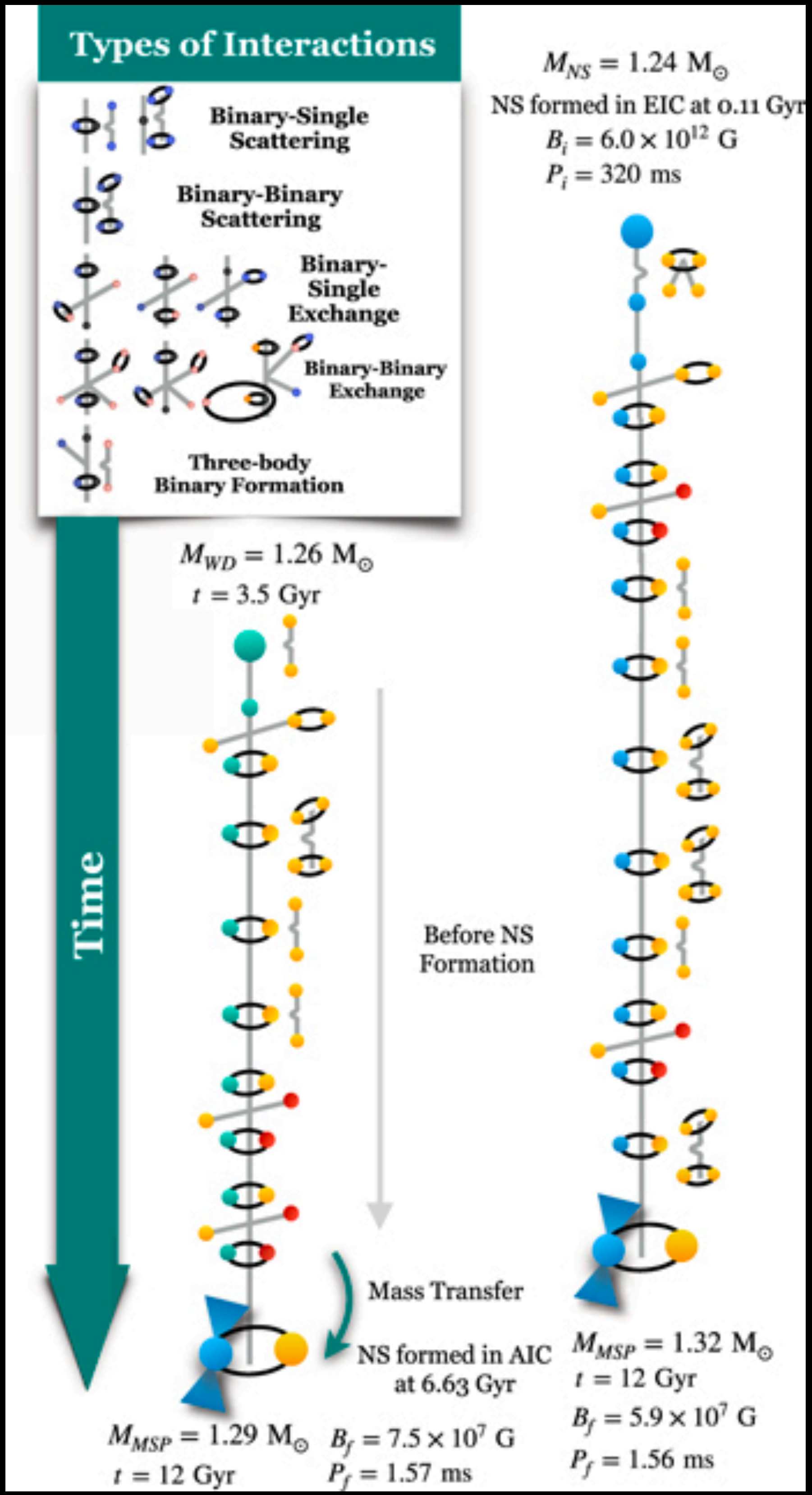

Ye et al. (2019)

GC MSP VS GF MSP

Lee et al. (2021 submitted)

GC MSP VS GF MSP

GC MSPs generally rotate ***slower*** than those in the GF.

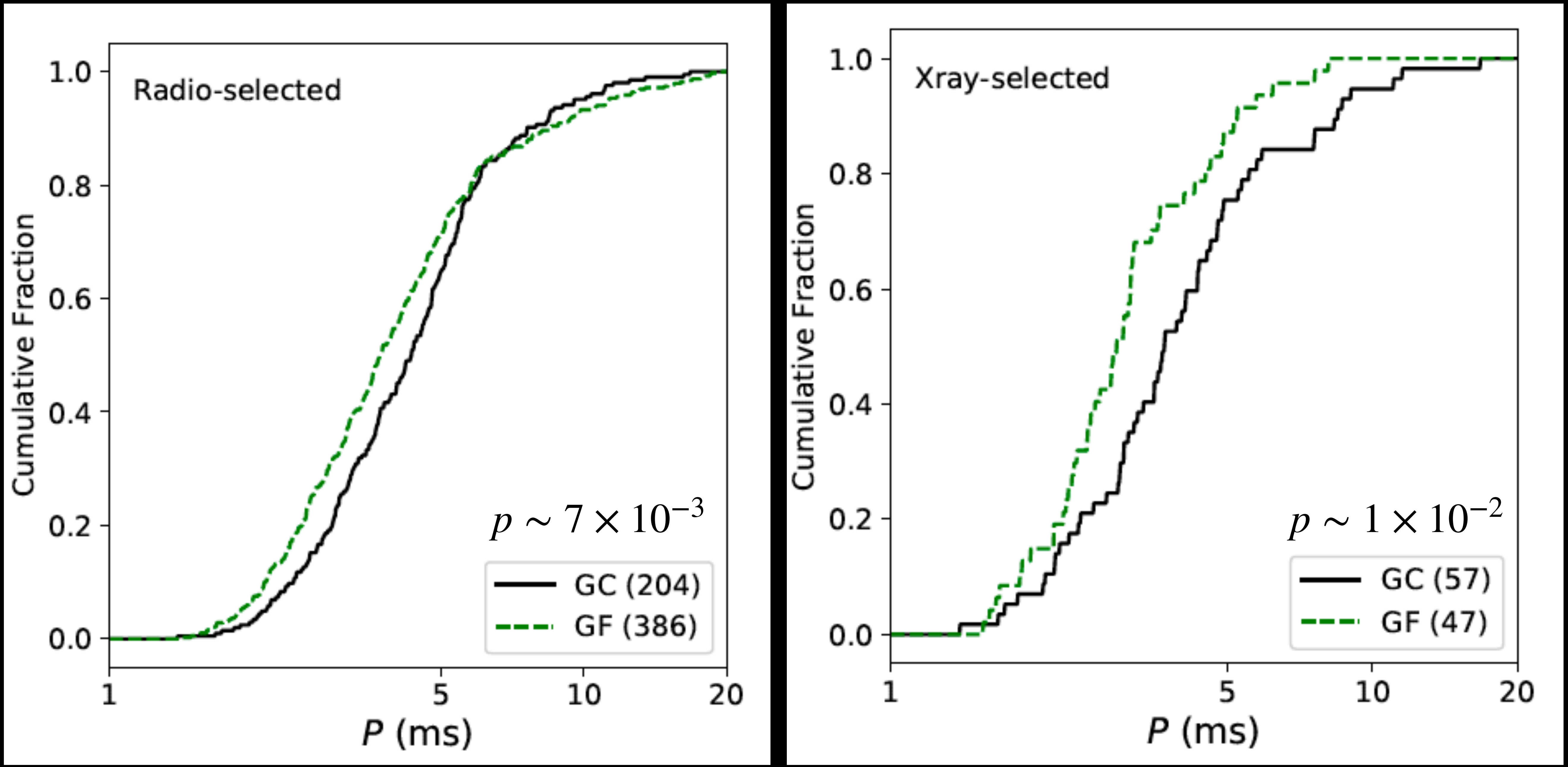

Lee et al. (2021 submitted)

GC MSP VS GF MSP

While X-ray observations tend to pick the MSPs with faster rotation in the GF, We do not find such selection effect in the GC MSP population.

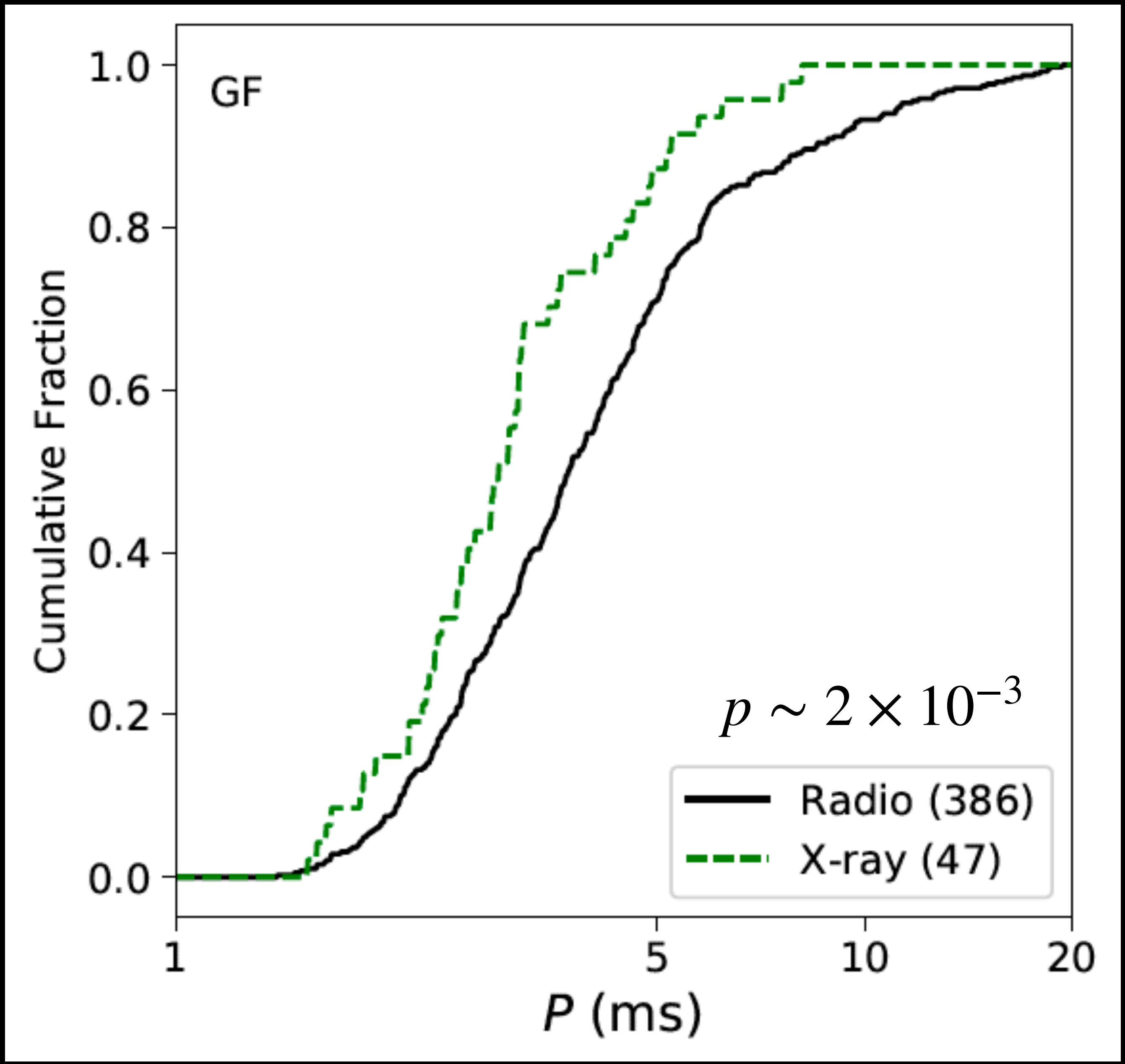

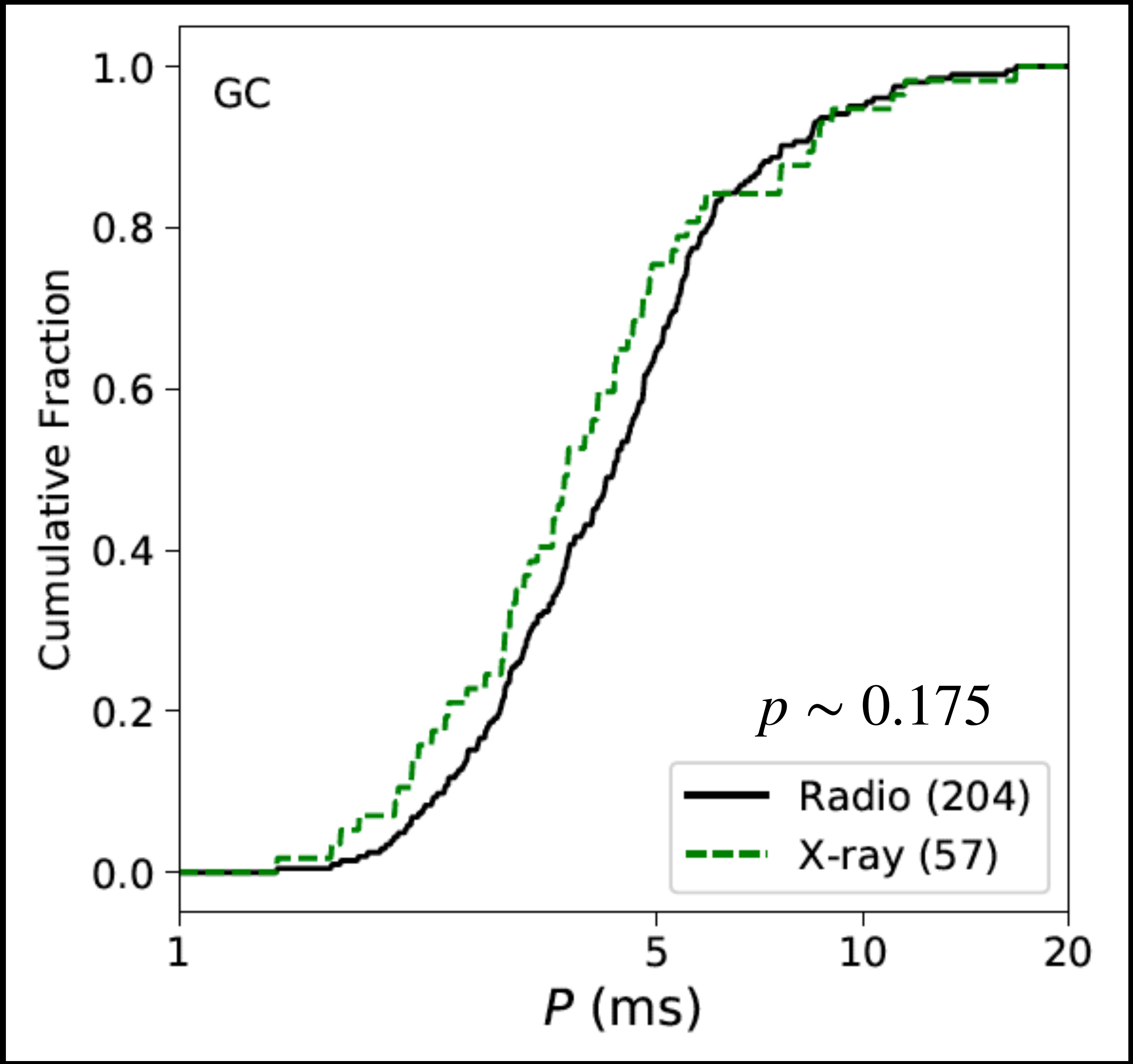

Lee et al. (2021 submitted)

GC MSP VS GF MSP

Surface magnetic field of GC MSPs are apparently stronger than those in the GF

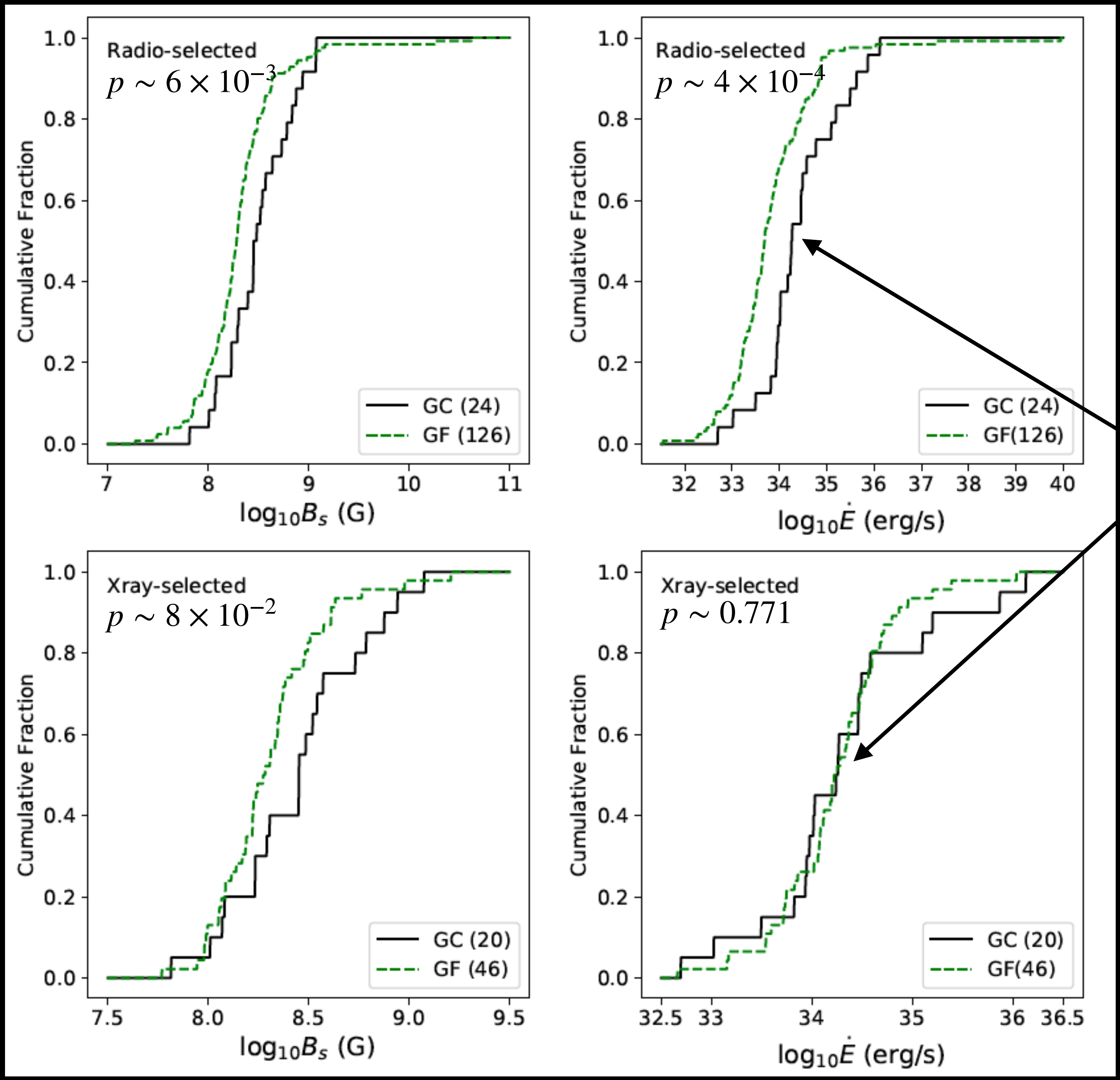

X-ray observations tend to pick more powerful MSPs in the GF.

Lee et al. (2021 submitted)

GC MSP VS GF MSP

For the GF MSP binaries, strong correlation is found between the rotation period and the orbital period. However, such correlation is absent in the GC MSPs.

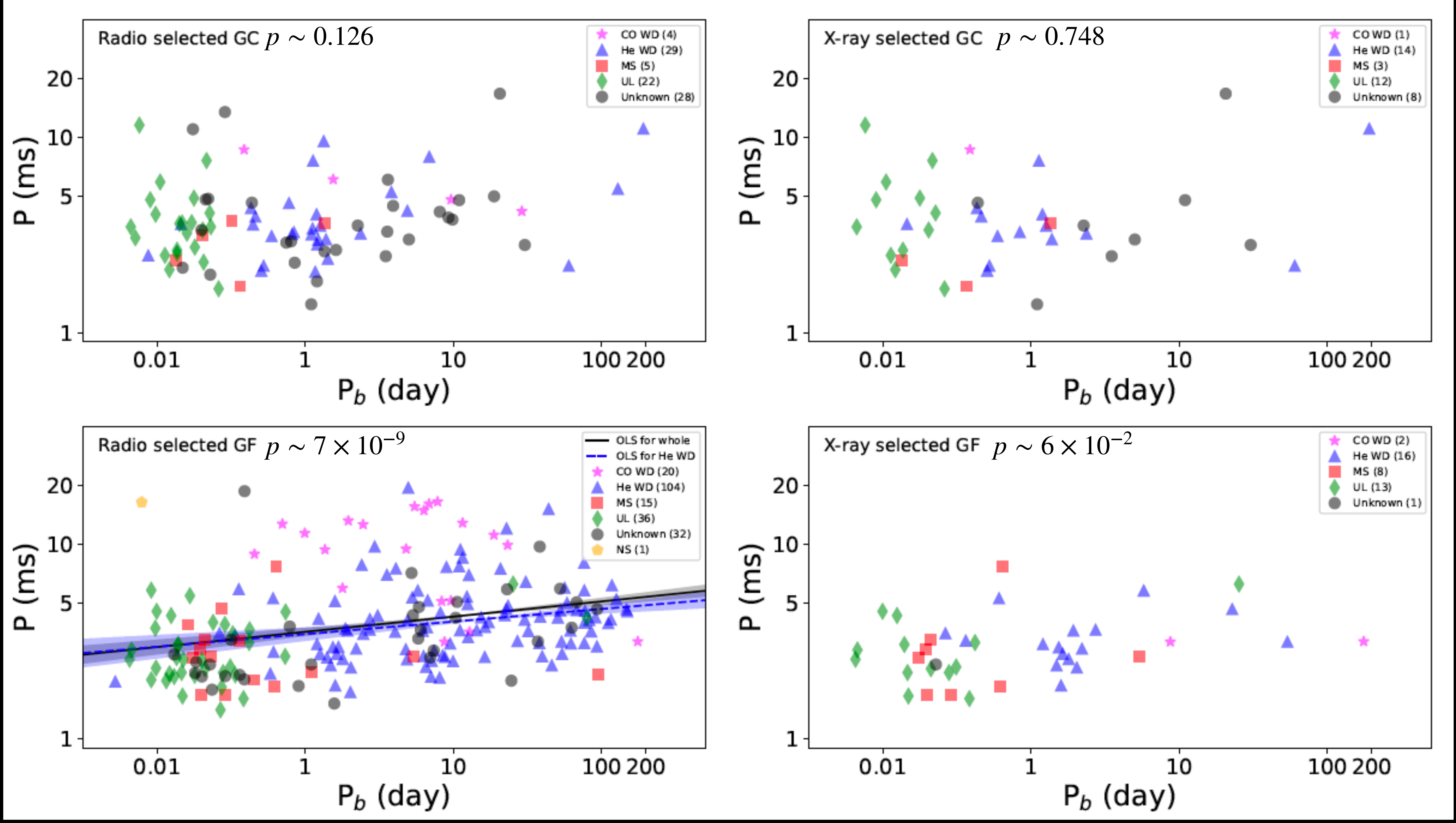

Lee et al. (2021 submitted)

GC MSP VS GF MSP

Distributions of X-ray luminosities and hardness are comparable in these two populations.

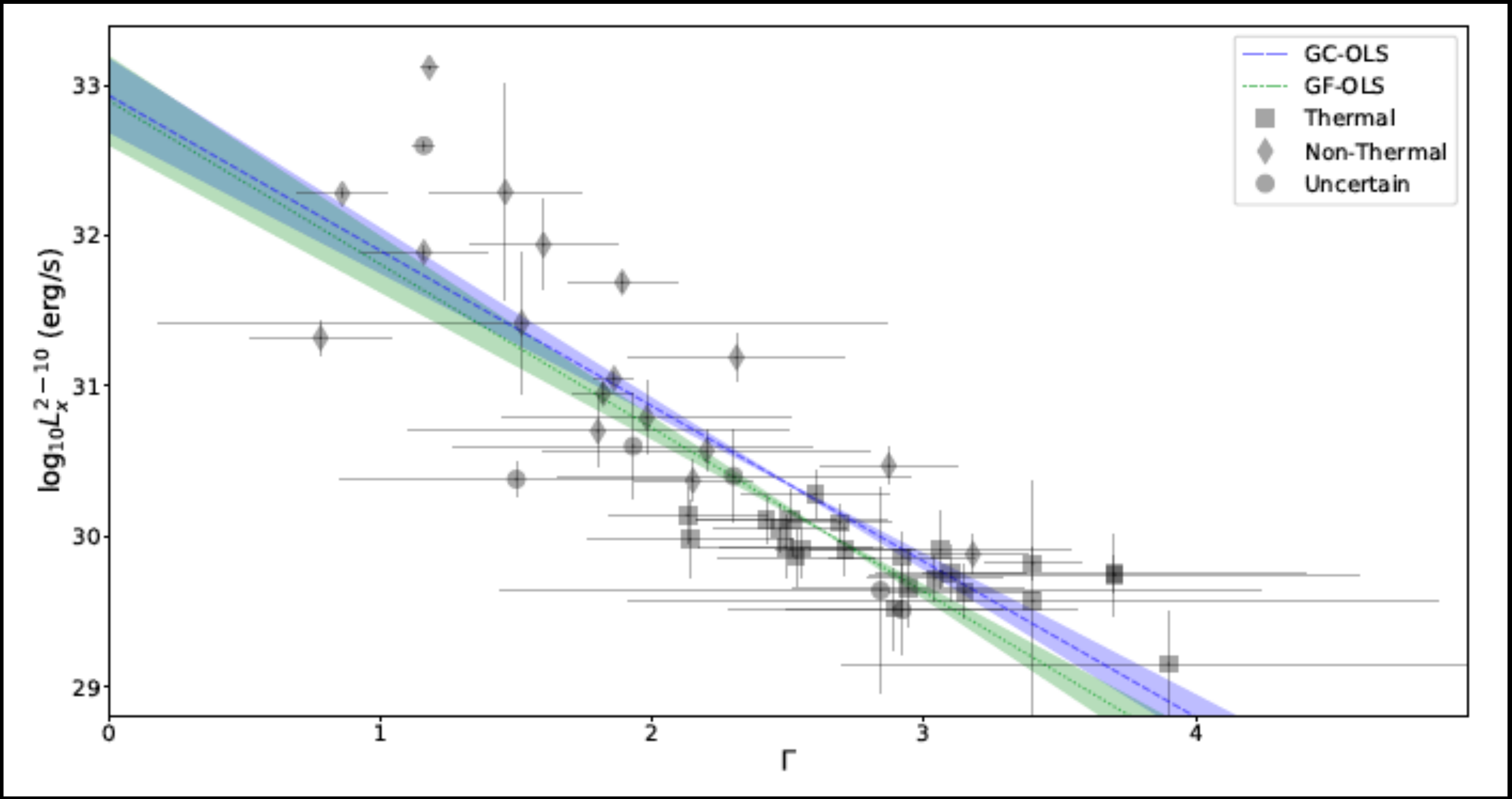

Lee et al. (2021 submitted)

GC MSP VS GF MSP

BUT their X-ray conversion efficiencies are significantly different

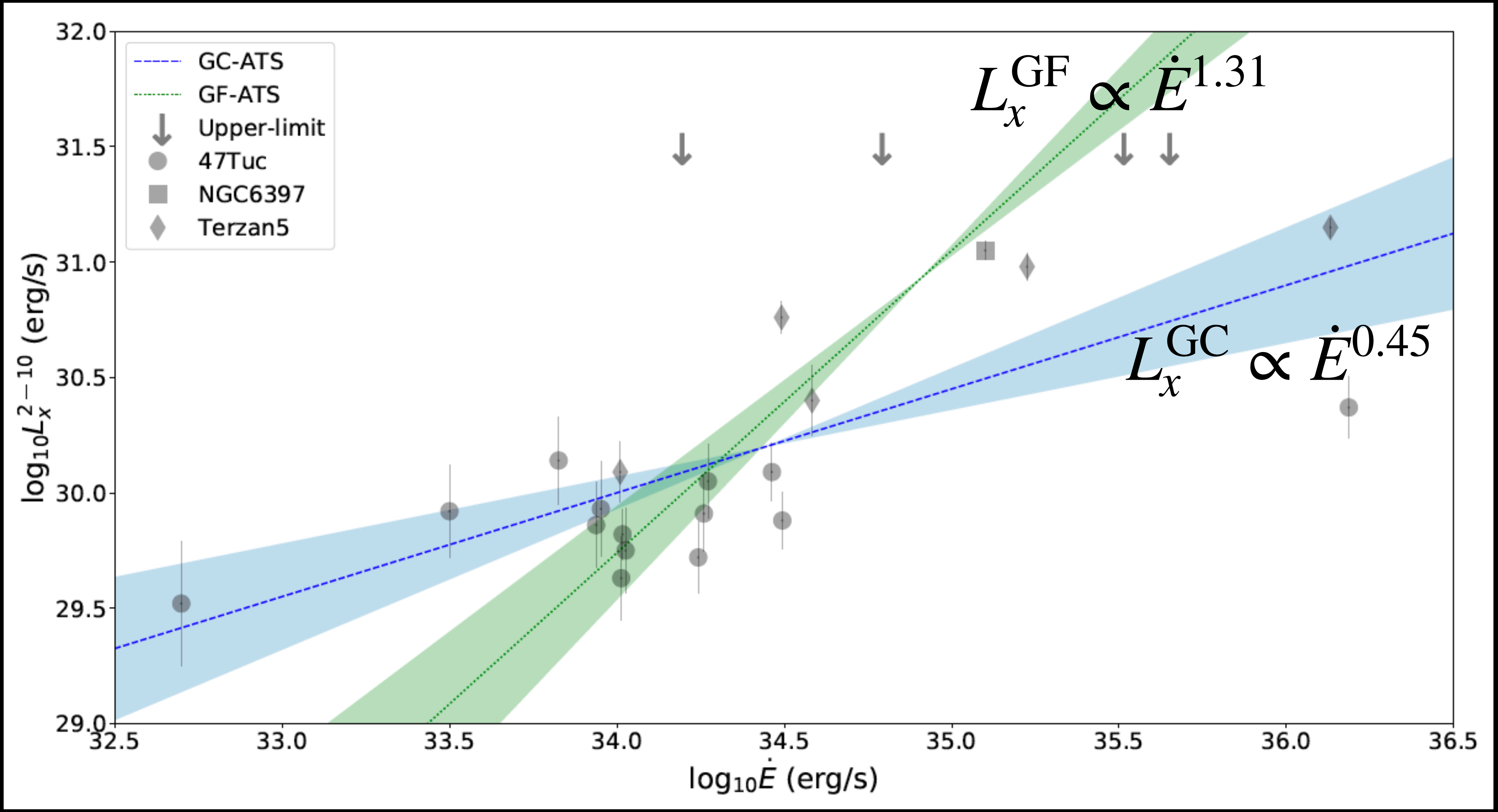

Lee et al. (2021 submitted)

GC MSP VS GF MSP

Disturbance on the recycling process by frequent stellar encounter

→ Mildly recycled MSPs in GC (i.e. slower rotation)

→ Halt the magnetic field decay (i.e. stronger surface field strength)

→ Absence of $P - P_b$ correlation

Halt the magnetic field decay → Enhanced polar cap heating by the back-flow magnetic pairs $L_x \propto J_{GJ} \sim \sqrt{\dot{E}}$ (i.e. Shallower $L_x - \dot{E}$ dependence)

→ Less prominent selection effect imposed by X-ray observations on GC MSPs

GAMMA-RAY FROM GC MSP

- It is difficult to resolve the gamma-ray emission from individual MSPs in GCs, except for two powerful cases:

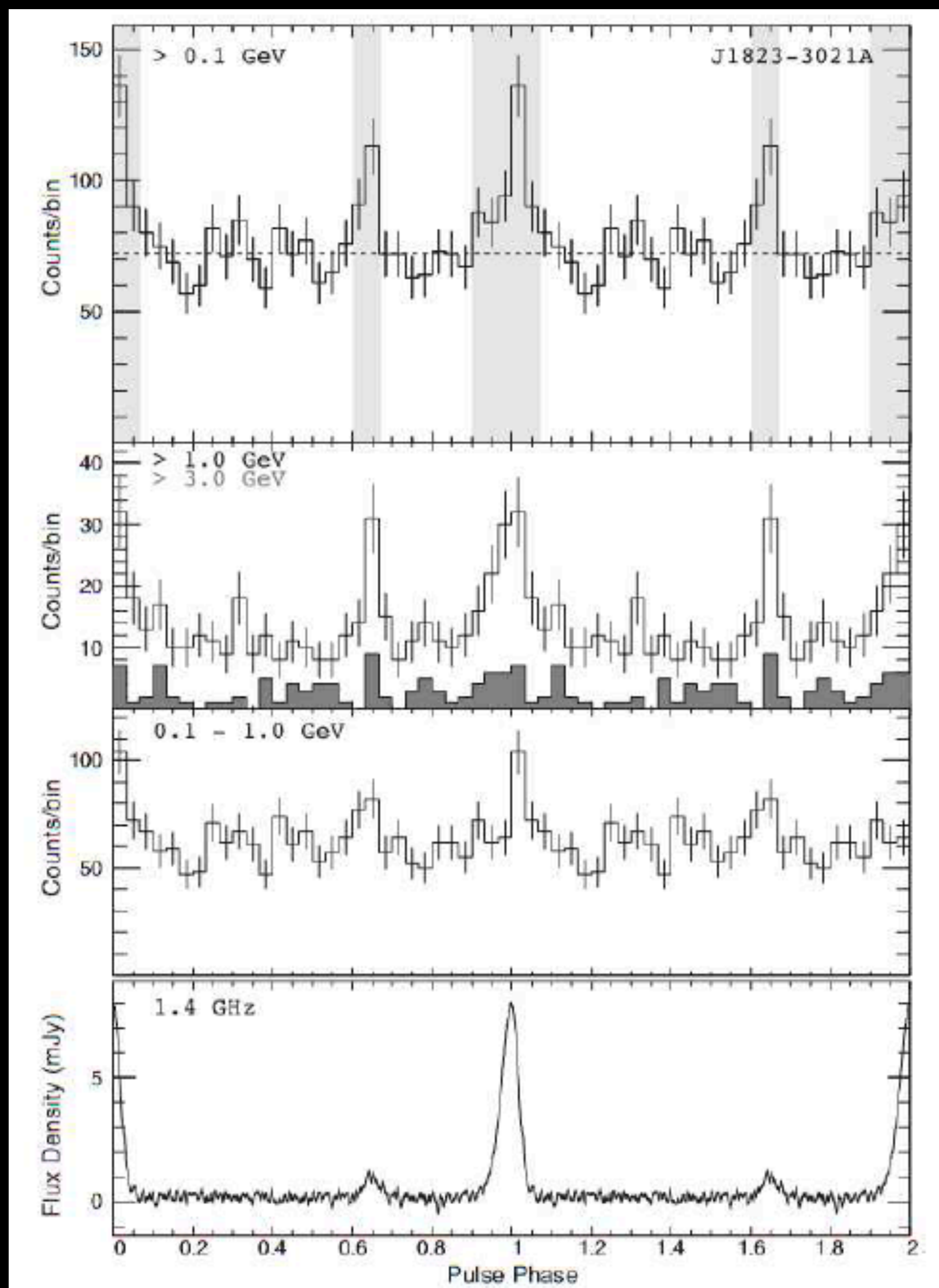

NGC 6624A (Freire et al. 2011)

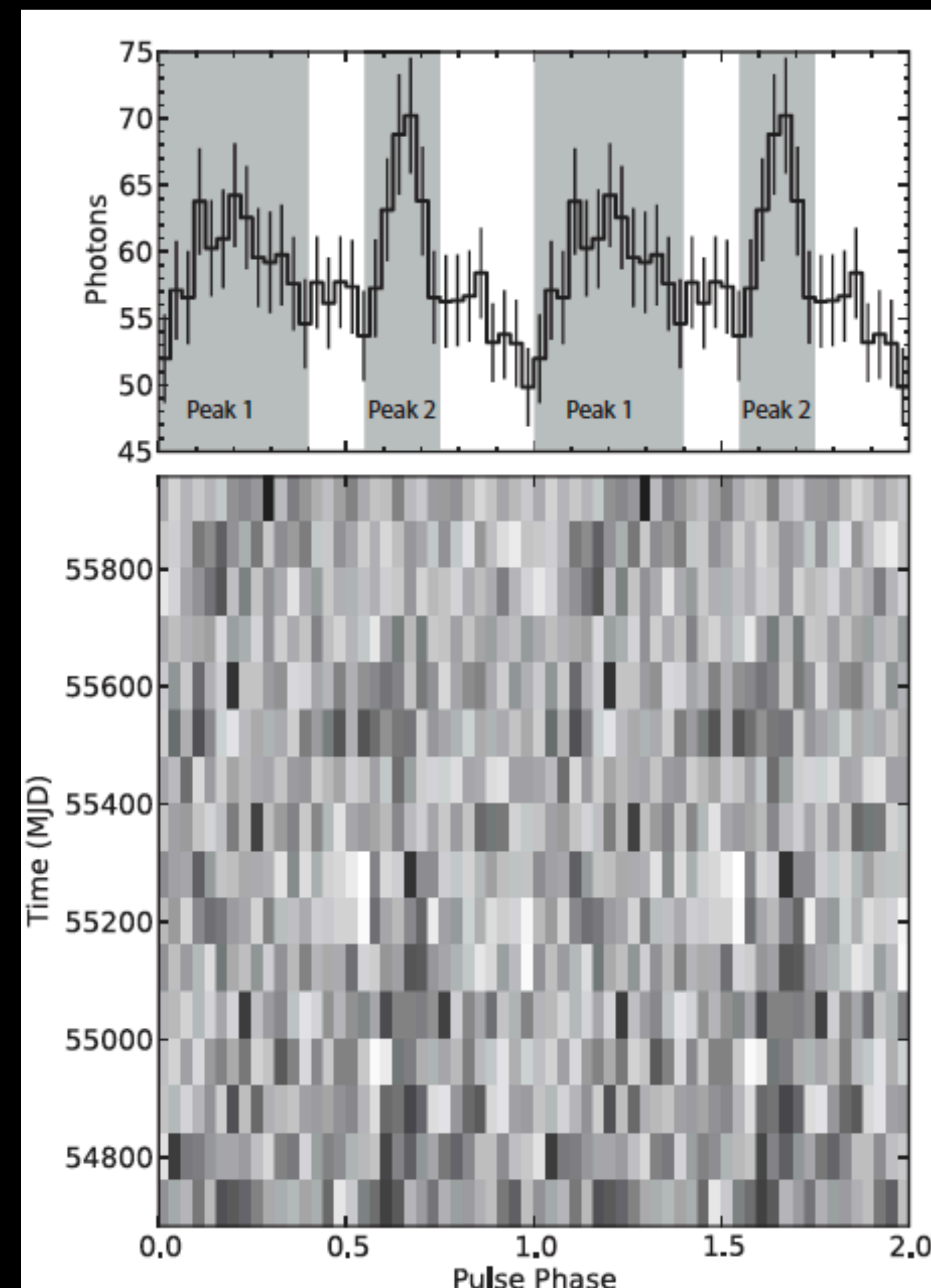

M28A (Wu, Hui et al. 2013)

GAMMA-RAY FROM GC MSP

- In updated 4FGL catalog, collective contributions of gamma-rays from the MSP populations have been detected in 25 GCs by Fermi LAT

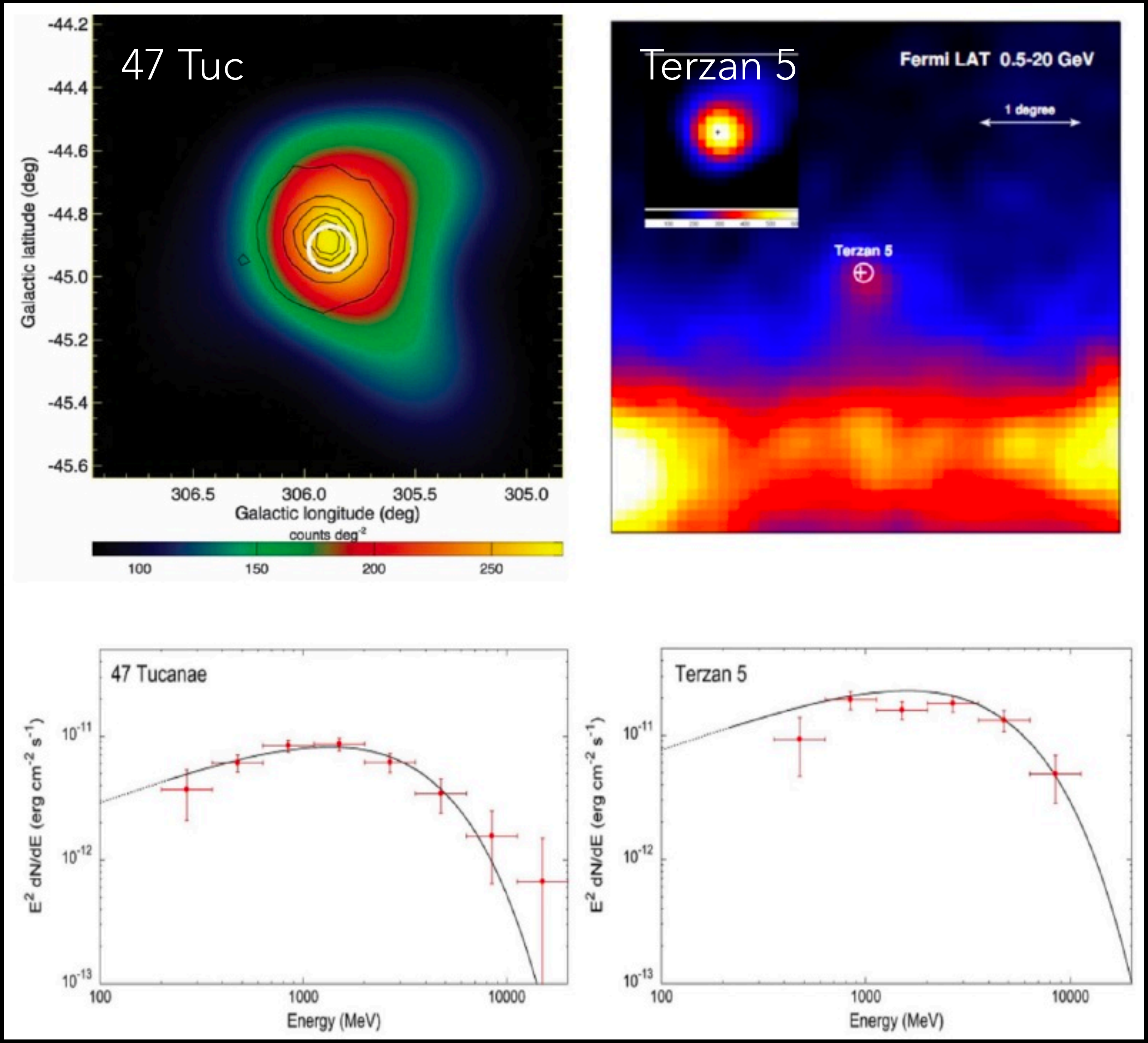

Abdo et al. (2009)　　Kong, Hui & Cheng (2010)

GAMMA-RAY FROM GC MSP

- Contributions can possibly come from (1) magnetospheric emission & (2) ICS between pulsar wind and ambient soft photon field

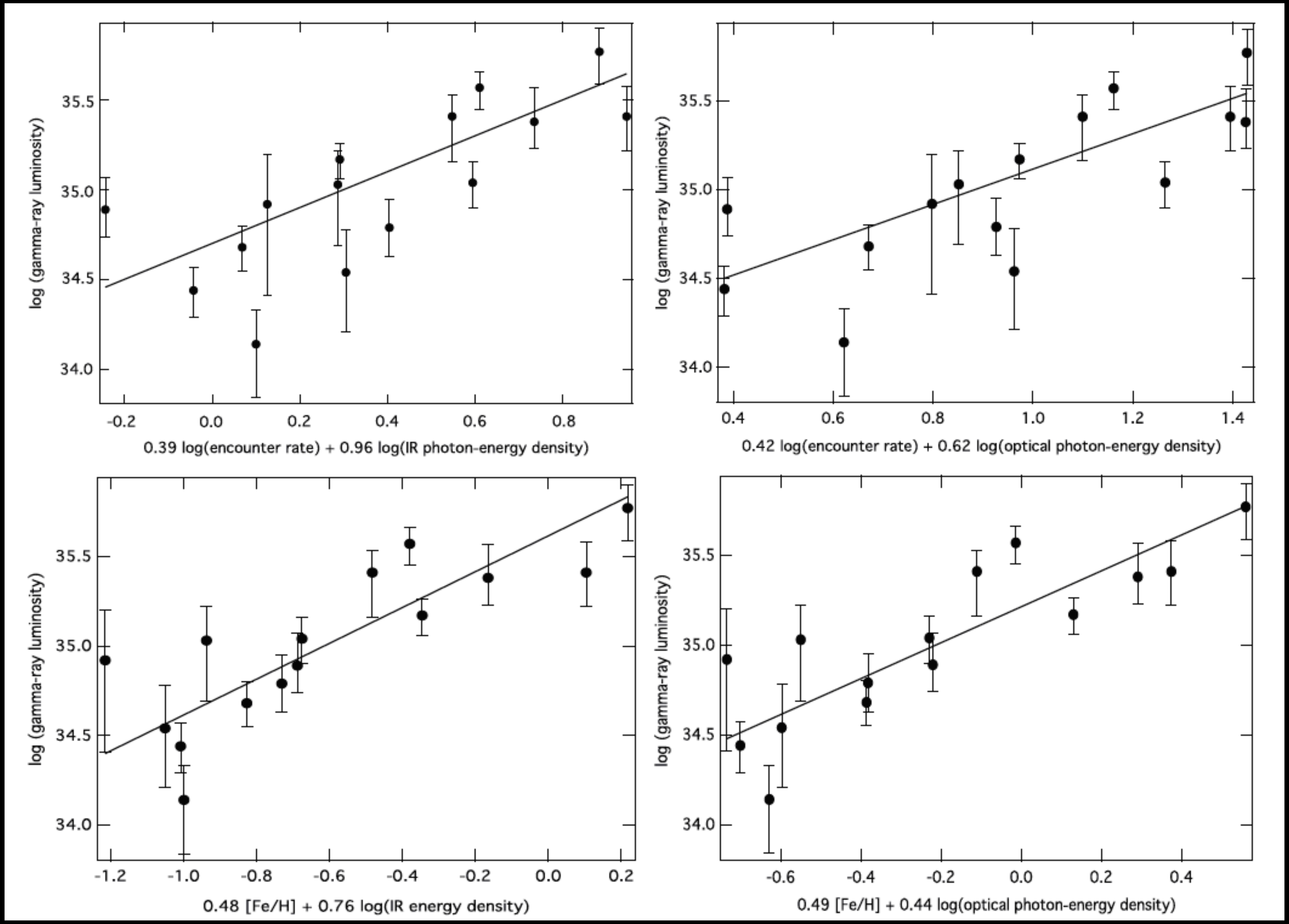

Hui et al. (2011)

GAMMA-RAY FROM GC MSP

- Recent study suggests that these two components can be comparable

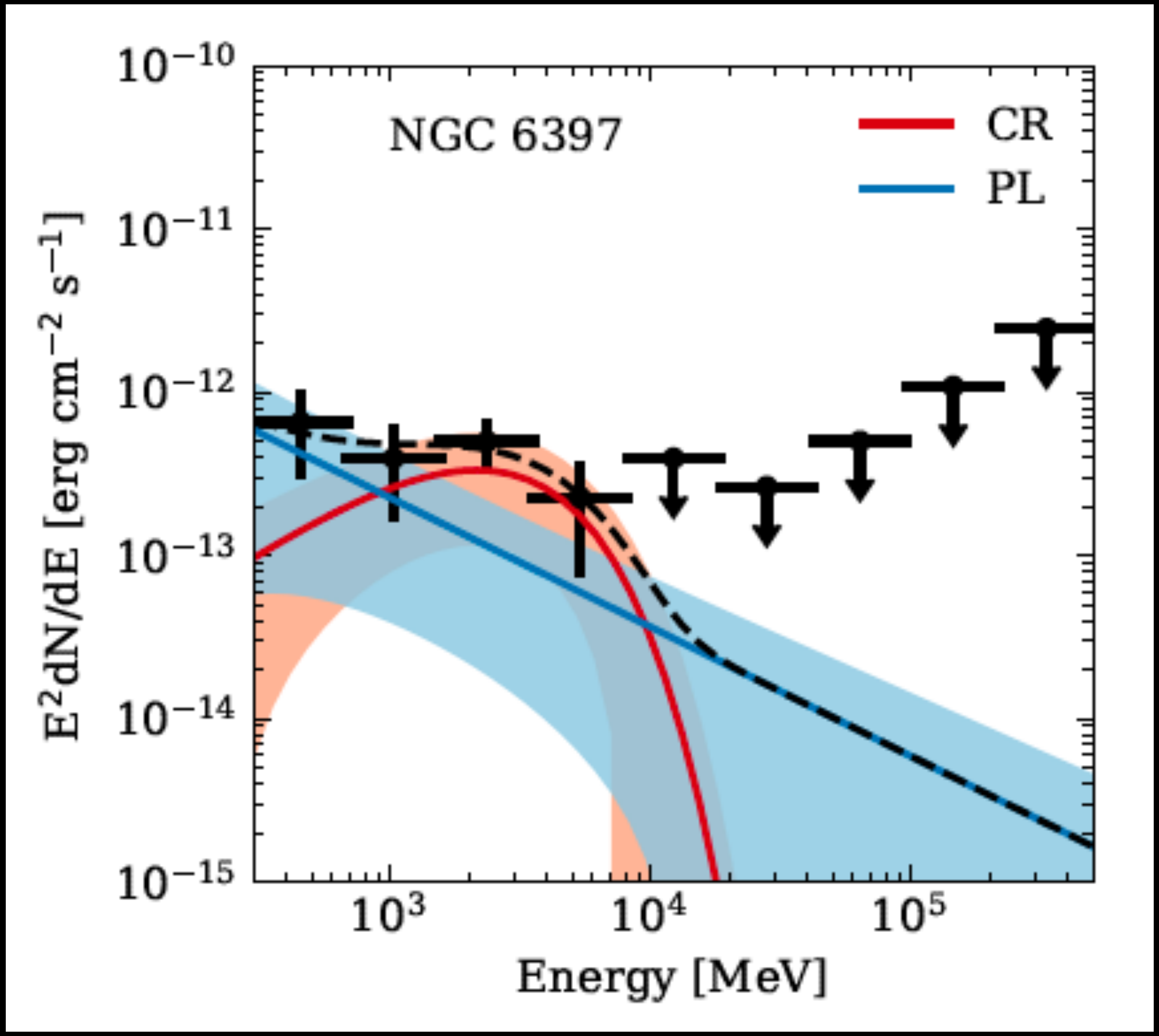

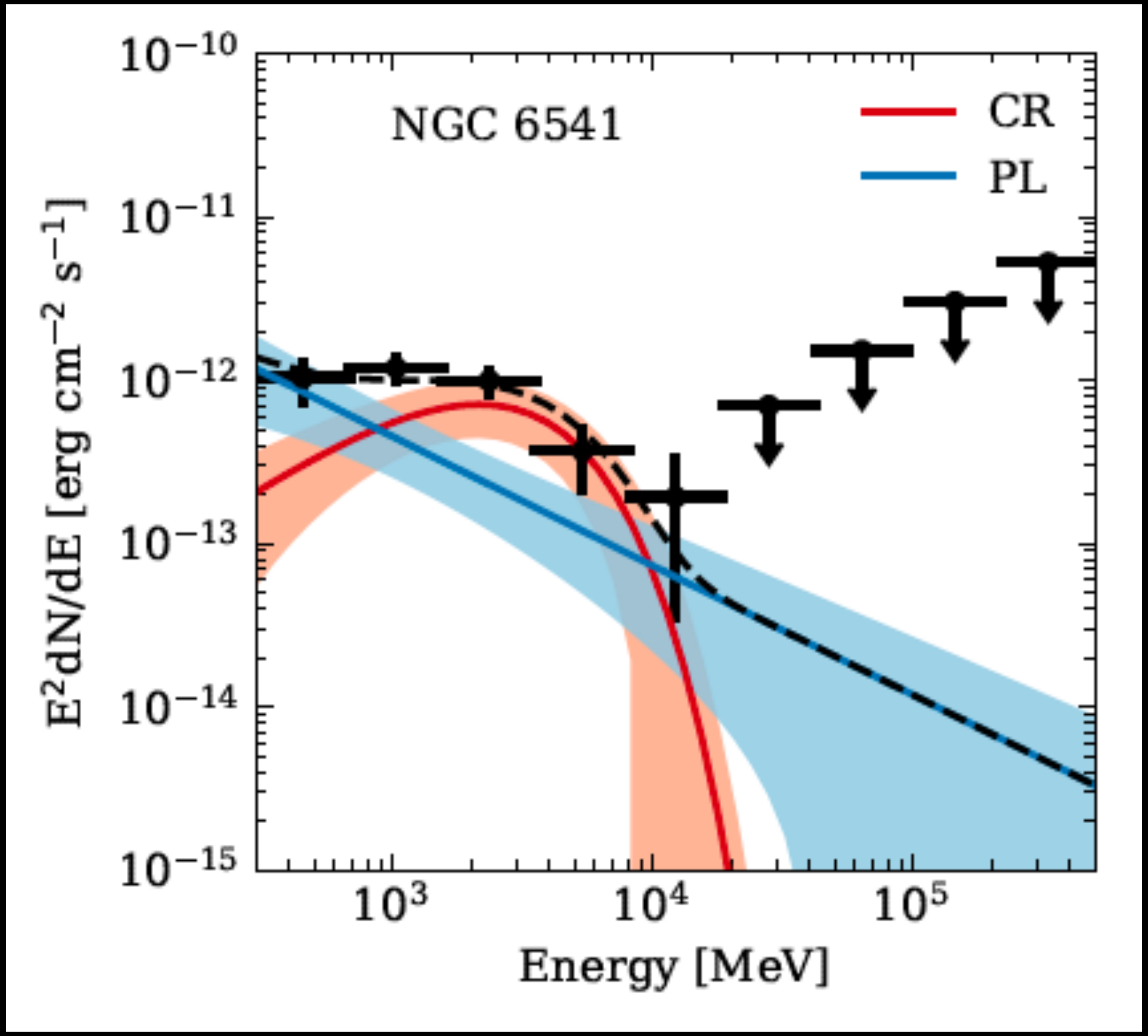

Song et al. (2021)

Can the pulsar wind contribute in VHE emission?

TEV FEATURE @ TERZAN 5

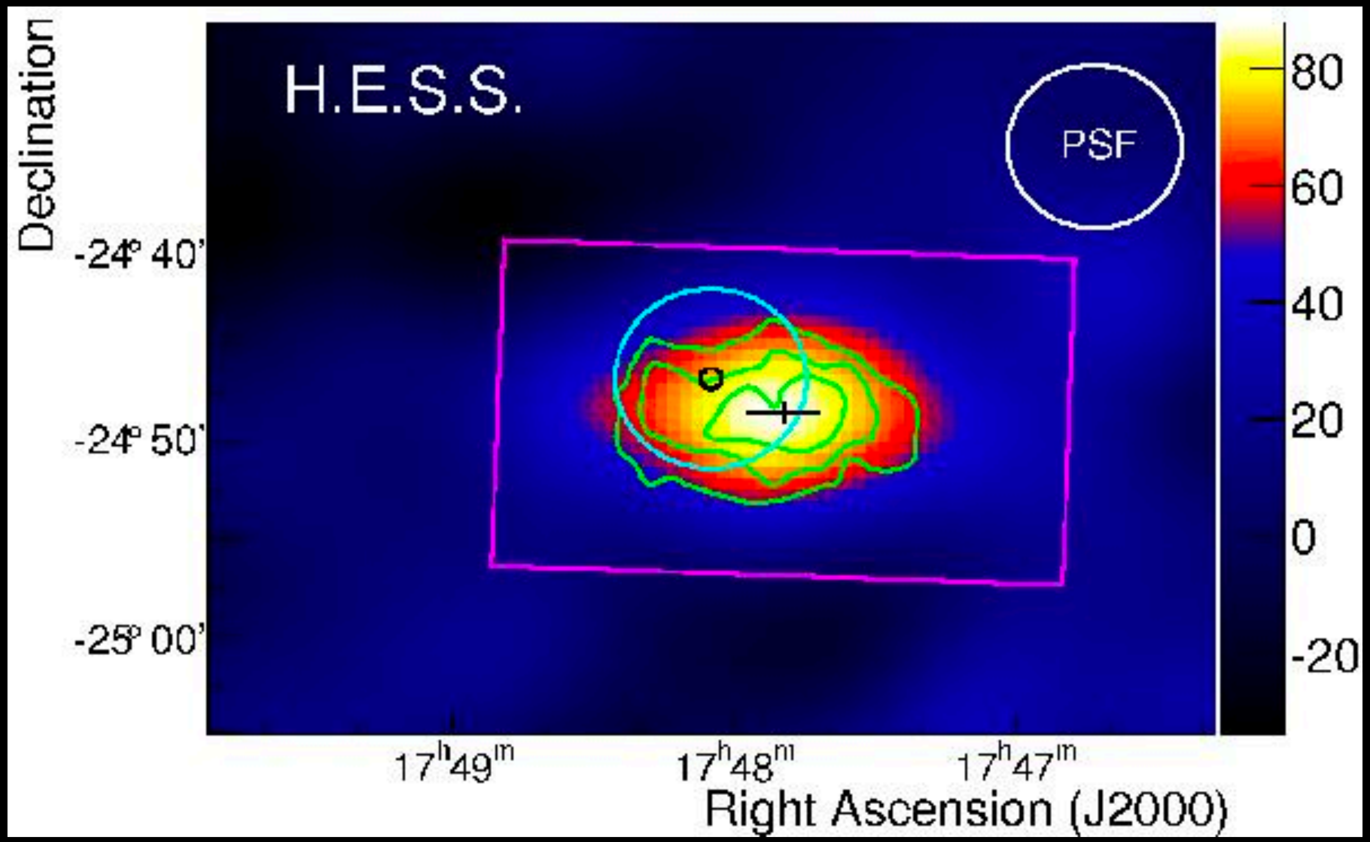

Abramowski et al. (2011)

- So far, VHE feature in the direction of Terzan 5 is the only plausible detection.
- Apparently extended
- Offset from the GC center
- Many different models have been proposed to explain its origin.

LIMITING FLUX (~1 TEV) OF GC

GC name	E_{th}[1] (TeV)	N_{ON}[2] (counts)	N_{OFF}[2] (counts)	$1/\alpha$[3]	sig.[4] (σ)	r[5] (°)	$F_{UL}(E > E_{th})$[6] ($ph\,cm^{-2}\,s^{-1}$)	$F_{UL}/F_{IC;GC}$[7]	$F_{UL}/F_{IC;IR,opt,CMB}$[7]
a) point-like source analysis									
NGC 104	0.72	72	941	18.2	2.6	–	1.9×10^{-12}	2.6×10^{-1}	2.1×10^{1}
NGC 6388	0.28	180	2365	14.9	1.6	–	1.5×10^{-12}	8.0×10^{-2}	1.6×10^{0}
NGC 7078	0.40	119	1988	15.0	−1.2	–	7.2×10^{-13}	1.9×10^{-1}	2.1×10^{1}
Terzan 6	0.28	202	8194	42.0	0.5	–	2.1×10^{-12}	7.3×10^{-1}	1.0×10^{0}
Terzan 10	0.23	76	2455	36.0	0.9	–	2.9×10^{-12}	4.3×10^{-1}	2.7×10^{-1}
NGC 6715	0.19	159	2361	15.2	0.3	–	9.3×10^{-13}	3.1×10^{-1}	1.3×10^{2}
NGC 362	0.59	18	533	33.0	0.4	–	2.4×10^{-12}	3.9×10^{0}	1.8×10^{2}
Pal 6	0.23	363	10 810	31.4	1.0	–	1.2×10^{-12}	1.3×10^{1}	1.1×10^{1}
NGC 6256	0.23	64	1869	27.4	−0.5	–	3.2×10^{-12}	1.8×10^{1}	2.9×10^{1}
Djorg 2	0.28	56	2387	39.4	−0.6	–	8.4×10^{-13}	1.0×10^{1}	1.0×10^{1}
NGC 6749	0.19	84	2633	29.3	−0.6	–	1.4×10^{-12}	2.5×10^{1}	4.1×10^{1}
NGC 6144	0.23	63	2196	30.8	−1.0	–	1.4×10^{-12}	3.8×10^{2}	1.1×10^{3}
NGC 288	0.16	647	24 148	38.5	0.8	–	5.3×10^{-13}	2.7×10^{2}	3.2×10^{3}
HP 1	0.23	67	2771	34.3	−1.6	–	1.5×10^{-12}	5.2×10^{2}	1.7×10^{2}
Terzan 9	0.33	89	2556	31.7	0.9	–	4.5×10^{-12}	2.6×10^{4}	9.0×10^{2}
b) extended source analysis									
NGC 104	"	293	2016	7.4	1.2	0.22	2.3×10^{-12}	2.3×10^{-1}	1.9×10^{1}
NGC 6388	"	253	2818	12.9	2.2	0.11	1.7×10^{-12}	9.2×10^{-2}	1.8×10^{0}
NGC 7078	"	161	2386	14.0	−0.7	0.11	1.1×10^{-12}	2.8×10^{-1}	3.1×10^{1}
Terzan 6	"	304	9802	34.2	1.0	0.12	2.4×10^{-12}	8.1×10^{-1}	1.2×10^{0}
Terzan 10	"	218	4134	19.0	0.0	0.18	3.6×10^{-12}	5.4×10^{-1}	3.4×10^{-1}
NGC 6715	"	159	2361	15.2	0.3	*	9.3×10^{-13}	3.1×10^{-1}	1.3×10^{2}
NGC 362	"	30	708	25.6	0.4	0.13	2.5×10^{-12}	4.0×10^{0}	1.8×10^{2}
Pal 6	"	1148	17 631	16.6	2.5	0.18	2.1×10^{-12}	2.4×10^{1}	1.9×10^{1}
NGC 6256	"	131	2524	20.4	0.6	0.13	3.9×10^{-12}	2.1×10^{1}	3.5×10^{1}
Djorg 2	"	137	3753	24.8	−1.2	0.16	9.7×10^{-13}	1.2×10^{1}	1.2×10^{1}
NGC 6749	"	168	3544	20.7	−0.3	0.14	2.1×10^{-12}	3.6×10^{1}	5.9×10^{1}
NGC 6144	"	120	2913	23.9	−0.2	0.13	2.5×10^{-12}	6.7×10^{2}	1.9×10^{3}
NGC 288	"	1030	30 767	30.7	0.8	0.13	6.1×10^{-13}	3.1×10^{2}	3.7×10^{3}
HP 1	"	67	2771	34.3	−1.6	*	1.5×10^{-12}	5.2×10^{2}	1.7×10^{2}
Terzan 9	"	206	3909	18.8	−0.1	0.16	4.1×10^{-12}	1.8×10^{4}	6.2×10^{2}
stacking analysis									
a)	0.23	2242	67 826	31.2	1.6	–	3.3×10^{-13}	$(5.4^{+16}_{-1.7}) \times 10^{-2}$	$(4.3^{+11}_{-1.4}) \times 10^{-1}$
b)	"	4425	92 037	21.6	2.4	–	4.5×10^{-13}	$(7.5^{+23}_{-2.4}) \times 10^{-2}$	$(5.9^{+17}_{-2.0}) \times 10^{-1}$

Abramowski et al. (2013)

CTA DETECTABILITY

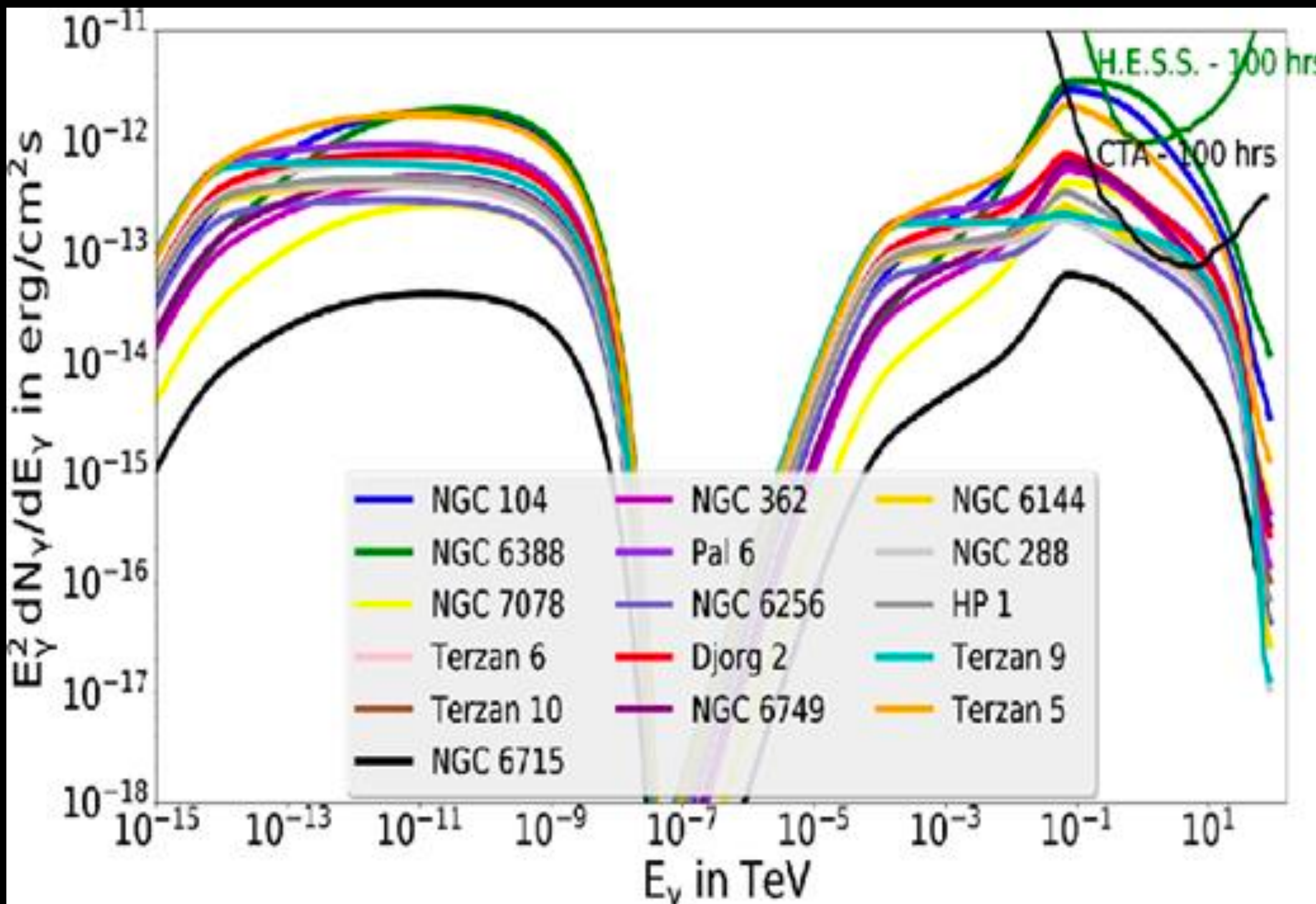

Ndiyavala et al. (2018)

- Using the limiting flux ~ 1 TeV imposed by HESS plus the limiting flux of diffuse X-rays, detectability of 16 GCs for CTA are predicted
- Furthermore, the authors expect CTA to detect more than half of the known GCs in Milky Way.
- BUT all these depend on (i) choice of parameters and (ii) the way of modeling (ALL GeV data are ignored in these calculations)

TEV HALO AROUND PULSARS

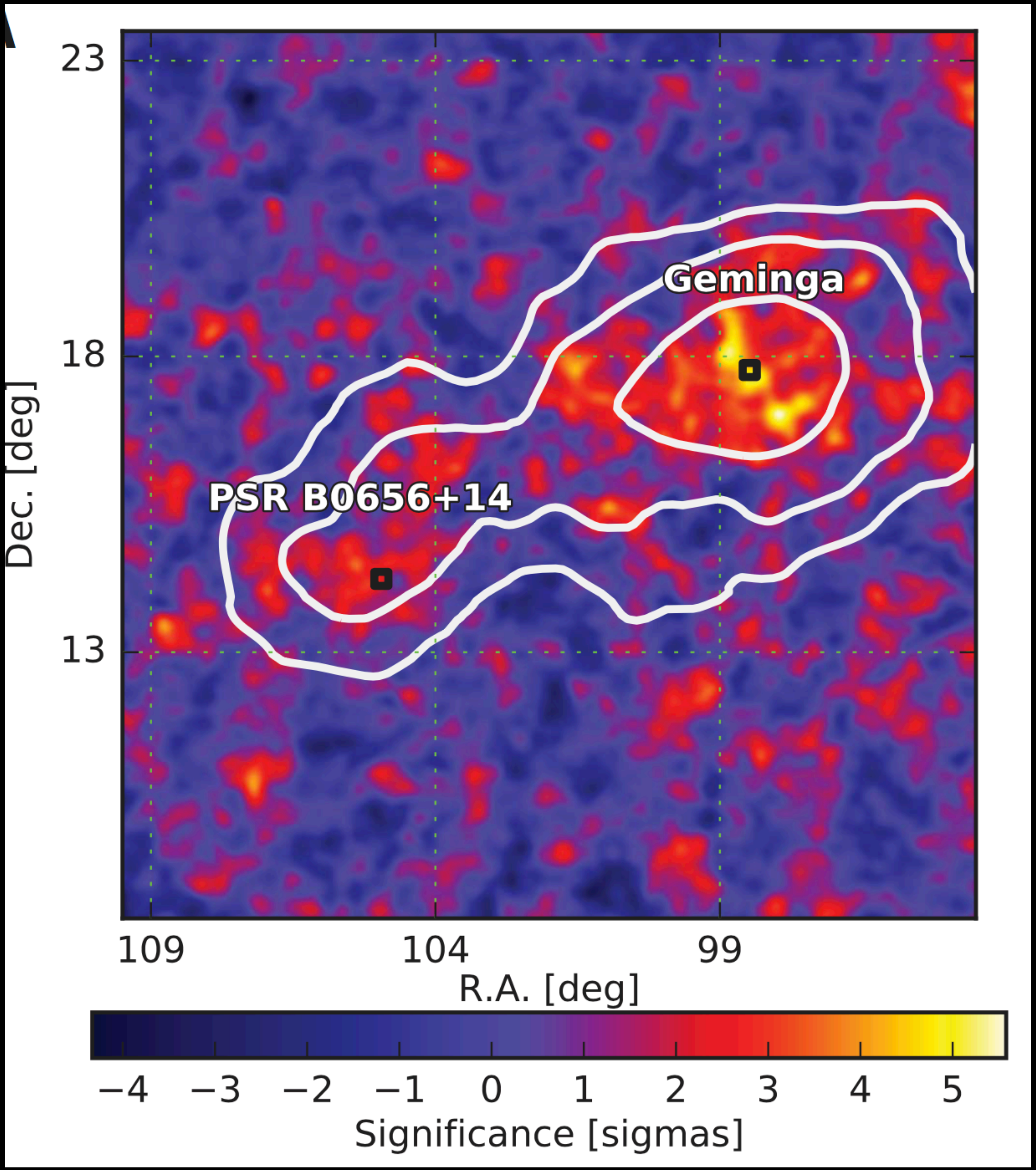

Abeysekara et al. (2017)

- Extended TeV emission is detected by HAWC and Milagro.
- 13 sigma in 1-50 TeV by HAWC.
- Spatial extent of ~few tens of pc.

TEV HALO AROUND PULSARS

- Indications for TeV emission around a few GF MSPs

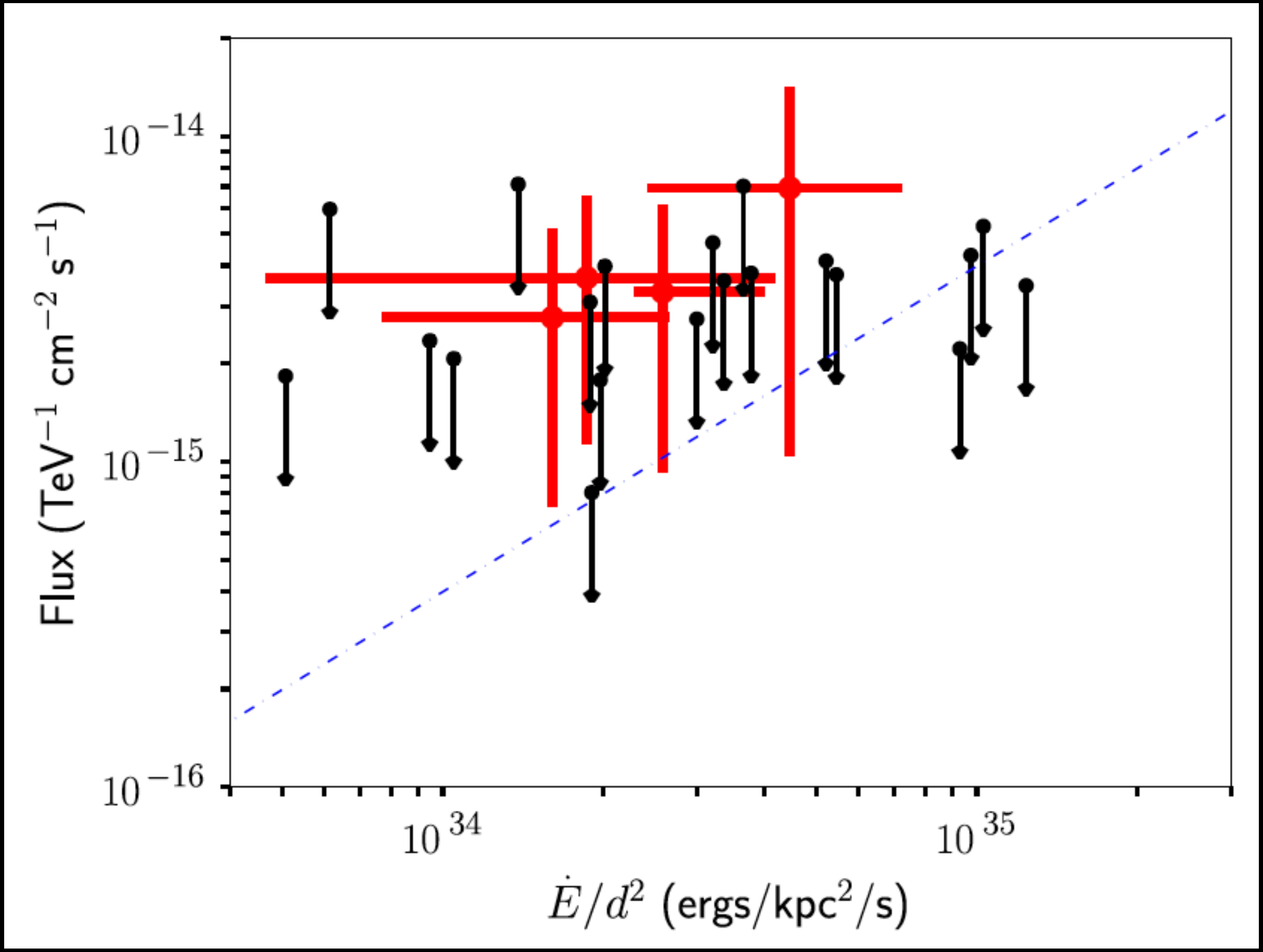

Hooper & Linden (2018, 2021)

TEV HALO AROUND PULSARS

- ~2-3 sigma indications for TeV emission at a few GF MSPs

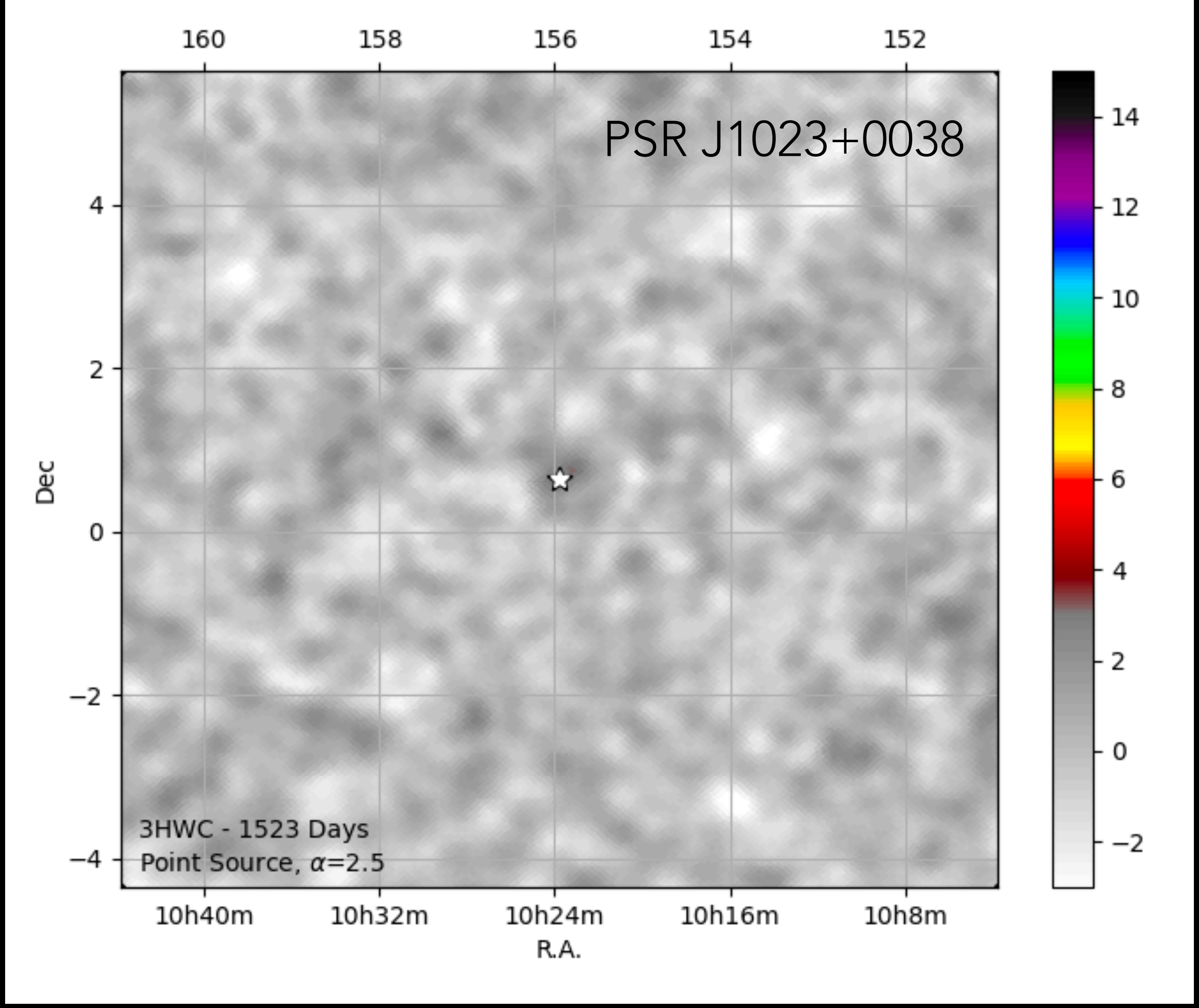

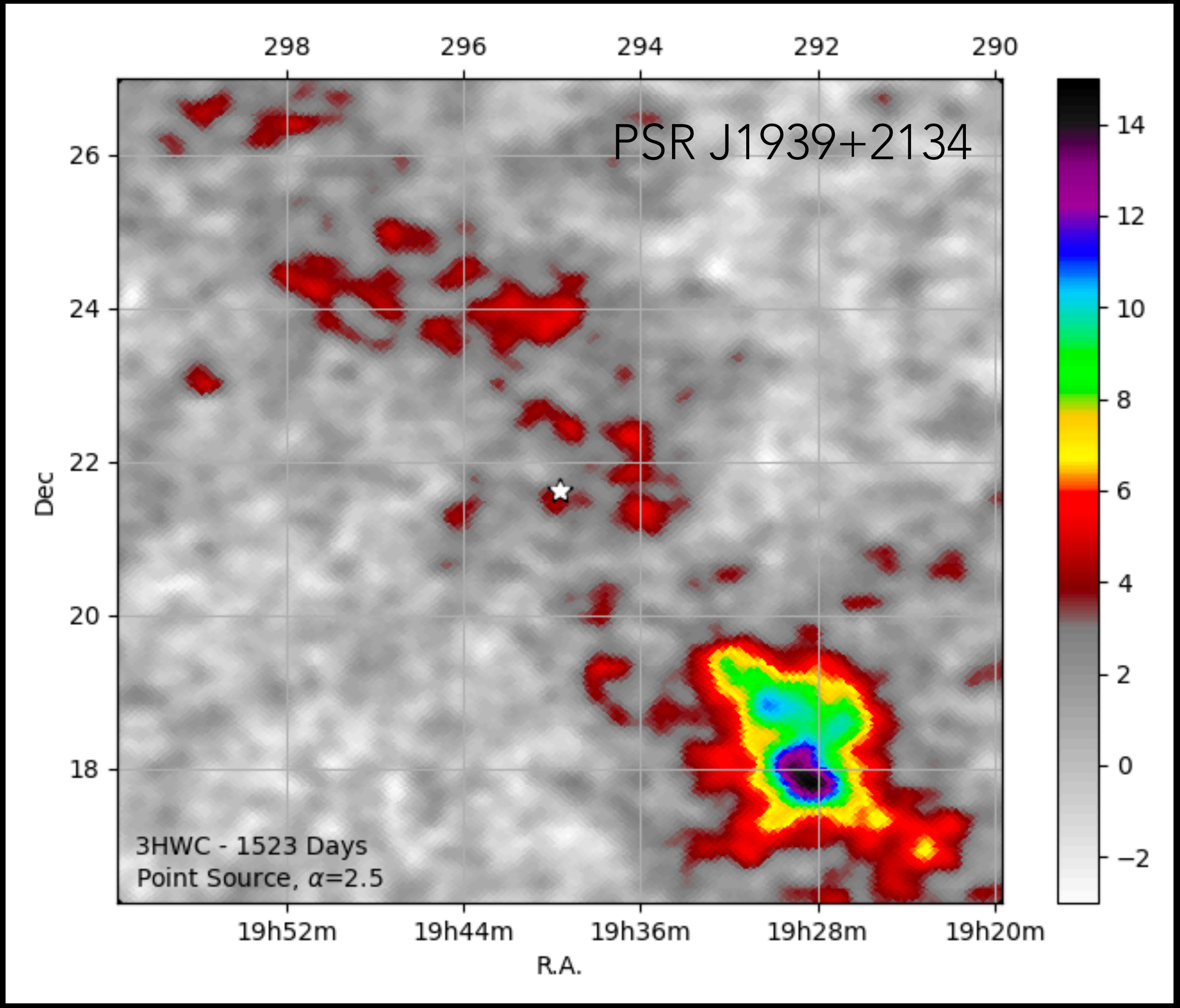

POSSIBILITY OF TEV HALO AROUND GC

- From the data in GeV, there is an evidence for the IC component from GCs which implies the contribution from the pulsar wind.
- And there are indications of TeV halos around some individual MSPs in the GF.
- Since a GC can house a large population of MSPs, it makes them as promising candidates for searching TeV halos around.

PATH FINDERS FOR TEV EMISSION AROUND GC

1. Search for extended X-ray features around GCs

2. Identifying the GCs with stronger IC component

3. Search for indication of TeV excess at GCs

DIFFUSE X-RAYS AROUND GC

- Magnetic field in the TeV halo is crucial in understanding the diffusion of pulsar wind particles
- e-/e+ gyrate in the magnetic field emit synchrotron radiation, which can give rise to a diffuse X-ray halo
- Detection/Non-detection of the X-ray halo can provide estimate/upper-limit of the magnetic field in the halo

DIFFUSE X-RAYS AROUND GC

- Using spatially-resolved imaging spectroscopy, it is possible to disentangle the diffuse X-rays in to multiple components

47 Tuc

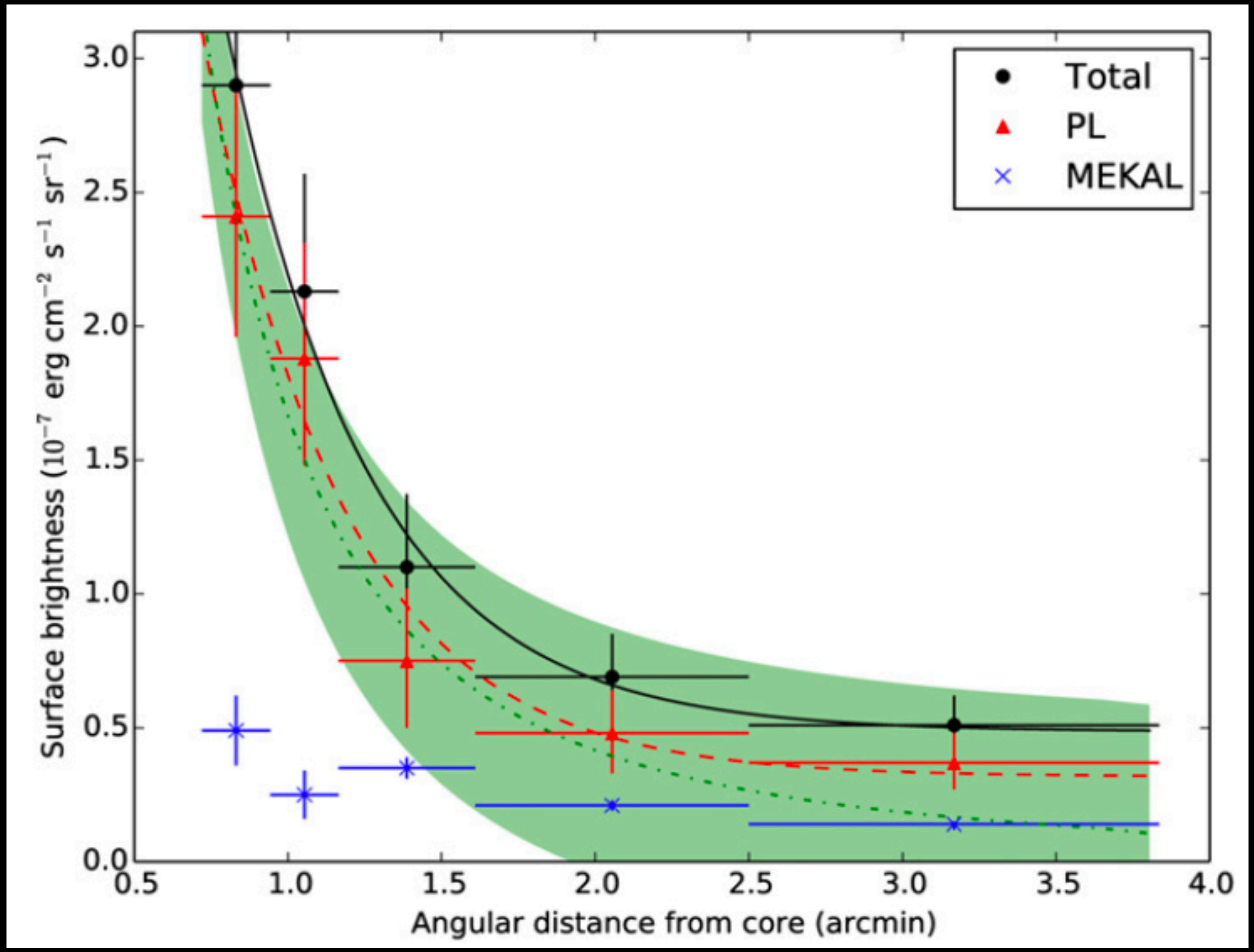

Wu, Hui et al. (2014)

Terzan 5

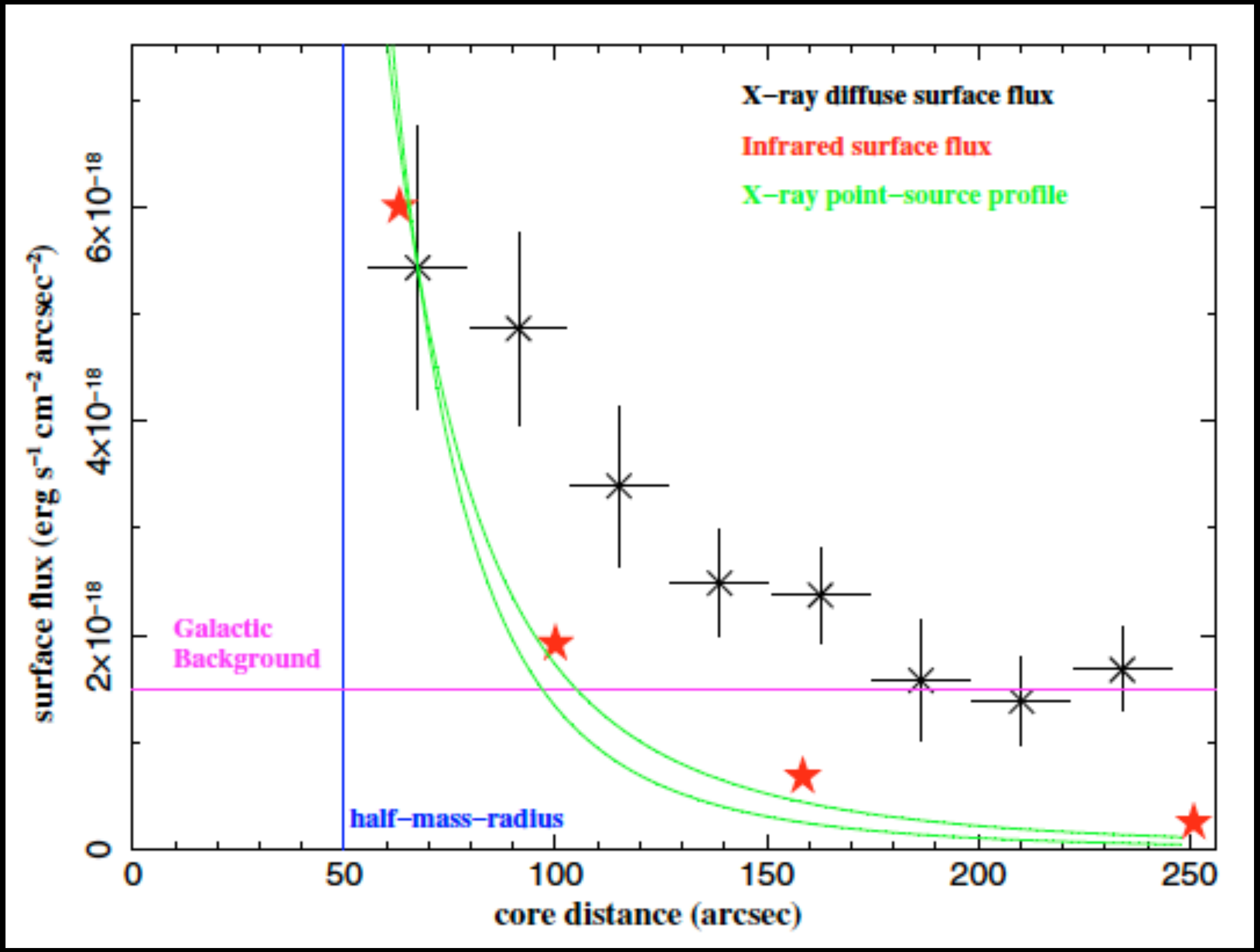

Eger, Domainko & Clapton (2010)

DIFFUSE X-RAYS AROUND GC

- There are plenty of archival X-ray data can be used for searching isotropic diffuse X-ray emission from GCs

Obs.ID	Start Date and Time (UTC)	Inst. (ACIS-)	Exposure time (ks)
NGC104 (47Tuc)			
953	2000-03-16T08:38:40	I	31.67
955	2000-03-16T18:32:00	I	31.67
2735	2002-09-29T16:57:56	S	65.24
2736	2002-09-30T13:24:28	S	65.24
2737	2002-10-02T18:50:07	S	65.24
2738	2002-10-11T01:41:55	S	65.24
16527	2014-09-05T04:38:37	S	40.88
15747	2014-09-09T19:32:57	S	50.40
16529	2014-09-21T07:55:51	S	24.70
15748	2014-10-02T06:17:00	S	16.24
16528	2015-02-02T14:23:34	S	40.28
NGC5139 (ω Cen)			
653	2000-01-24T02:13:58	I	25.03
1519	2000-01-25T04:32:36	I	43.59
13727	2012-04-16T06:18:36	I	48.53
13726	2012-04-17T08:16:43	I	173.74
NGC6121 (M4)			
946	2000-06-30T04:24:23	S	25.82
7447	2007-07-06T05:26:35	S	45.46
7446	2007-09-18T02:47:24	S	47.93
NGC6205 (M13)			
7290	2006-03-09T23:01:13	S	27.89
5436	2007-03-11T06:19:34	S	26.80
NGC6266 (M62)			
2677	2002-05-12T09:12:42	S	62.27
15761	2014-05-05T19:18:39	S	82.09
NGC6397			
79	2000-07-31T15:30:29	I	48.34
2668	2002-05-13T19:17:40	S	28.10
2669	2002-05-15T18:53:27	S	26.66
7461	2007-06-22T21:44:15	S	88.90
7460	2007-07-16T06:21:36	S	147.71
NGC6440			
947	2000-07-04T13:28:39	S	23.28
3799	2003-06-27T08:57:31	S	24.05
10060	2009-07-28T15:05:44	S	49.11
NGC6656 (M22)			
5437	2005-05-24T21:21:23	S	15.82
14609	2014-05-22T19:39:17	S	84.86
NGC6838 (M71)			
5434	2004-12-20T15:18:45	S	52.45

Obs.ID	Start Date and Time (UTC)	Inst. (ACIS-)	Exposure time (ks)
Terzan5			
3798	2003-07-13T13:22:45	S	39.34
10059	2009-07-15T17:19:56	S	36.26
13225	2011-02-14T09:05:34	S	29.67
13252	2011-04-29T17:06:31	S	39.54
13705	2011-09-05T16:54:24	S	13.87
14339	2011-09-08T03:32:23	S	34.06
13706	2012-05-13T17:58:45	S	46.46
14475	2012-09-17T16:10:24	S	30.50
14476	2012-10-28T03:14:38	S	28.60
14477	2013-02-05T04:16:59	S	28.60
14625	2013-02-22T08:22:32	S	49.20
15615	2013-02-23T10:17:02	S	84.16
14478	2013-07-16T21:12:59	S	28.60
14479	2014-07-15T05:23:11	S	28.60
16638	2014-07-17T11:48:31	S	71.60
15750	2014-07-20T16:41:37	S	22.99
17779	2016-07-13T18:41:43	S	68.85
18881	2016-07-15T11:50:35	S	64.71
NGC6626 (M28)			
2684	2002-07-04T18:02:19	S	12.75
2685	2002-08-04T23:46:25	S	13.51
2683	2002-09-09T16:55:03	S	14.11
9132	2008-08-07T20:45:43	S	142.26
9133	2008-08-10T23:50:24	S	54.46
14616	2013-04-28T19:37:19	S	14.79
16748	2015-05-30T02:34:33	S	29.66
16749	2015-08-07T20:13:25	S	29.55
16750	2015-11-07T16:05:40	S	29.57
NGC6752			
948	2000-05-15T04:36:02	S	29.47
6612	2006-02-10T22:48:48	S	37.97
19014	2017-07-02T03:27:25	S	98.81
19013	2017-07-24T09:33:12	S	43.20
20121	2017-07-25T17:04:15	S	18.26
20122	2017-07-29T09:00:43	S	67.22
20123	2017-07-30T23:53:18	S	49.46

Lee et al. (2021 submitted)

DIFFUSE X-RAYS AROUND GC

- The large FoV (~ 1 deg) of eROSITA can be used for searching diffuse features to a a much larger extent

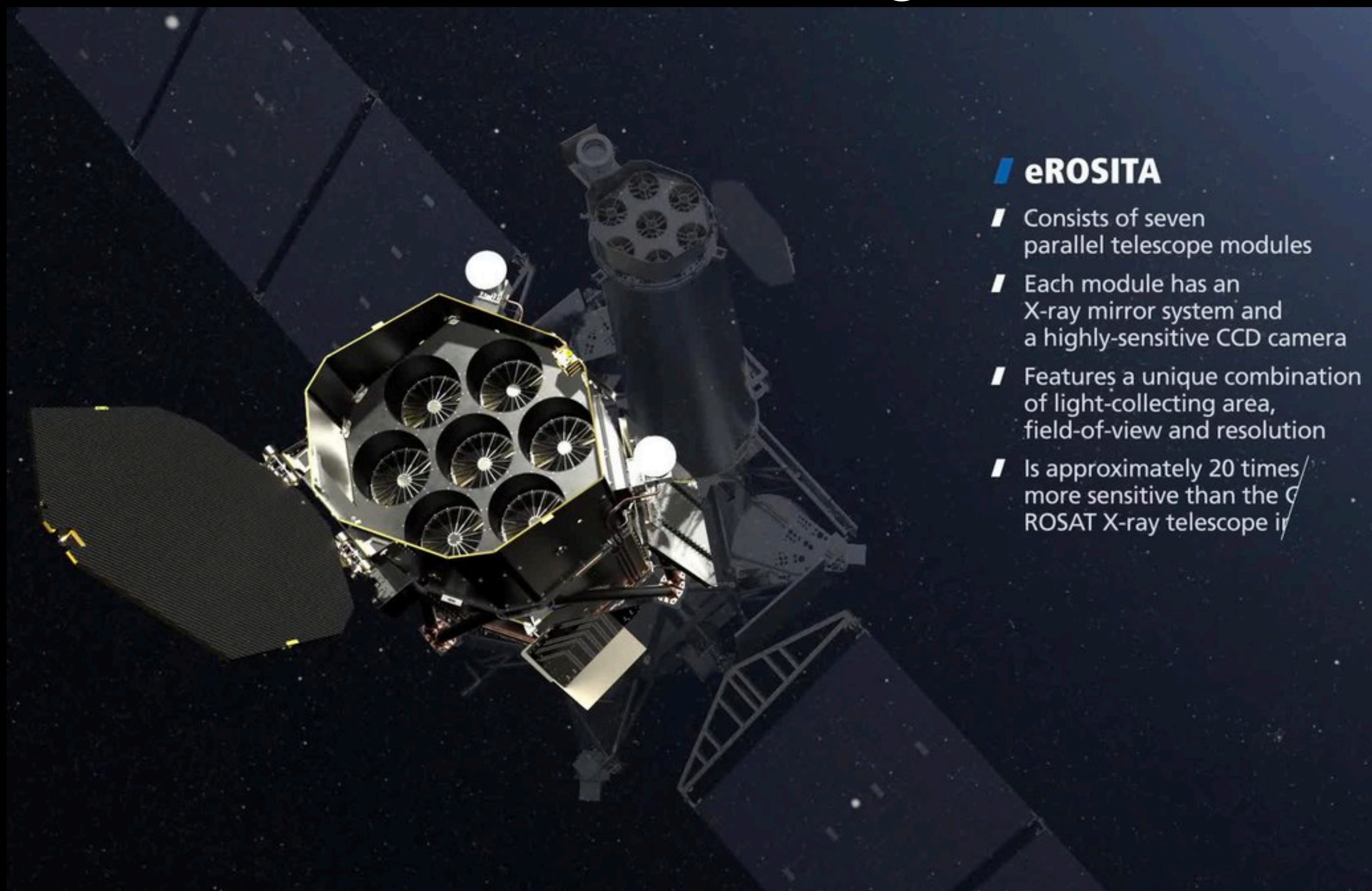

FoV with ~42′ radius @ 47 Tuc

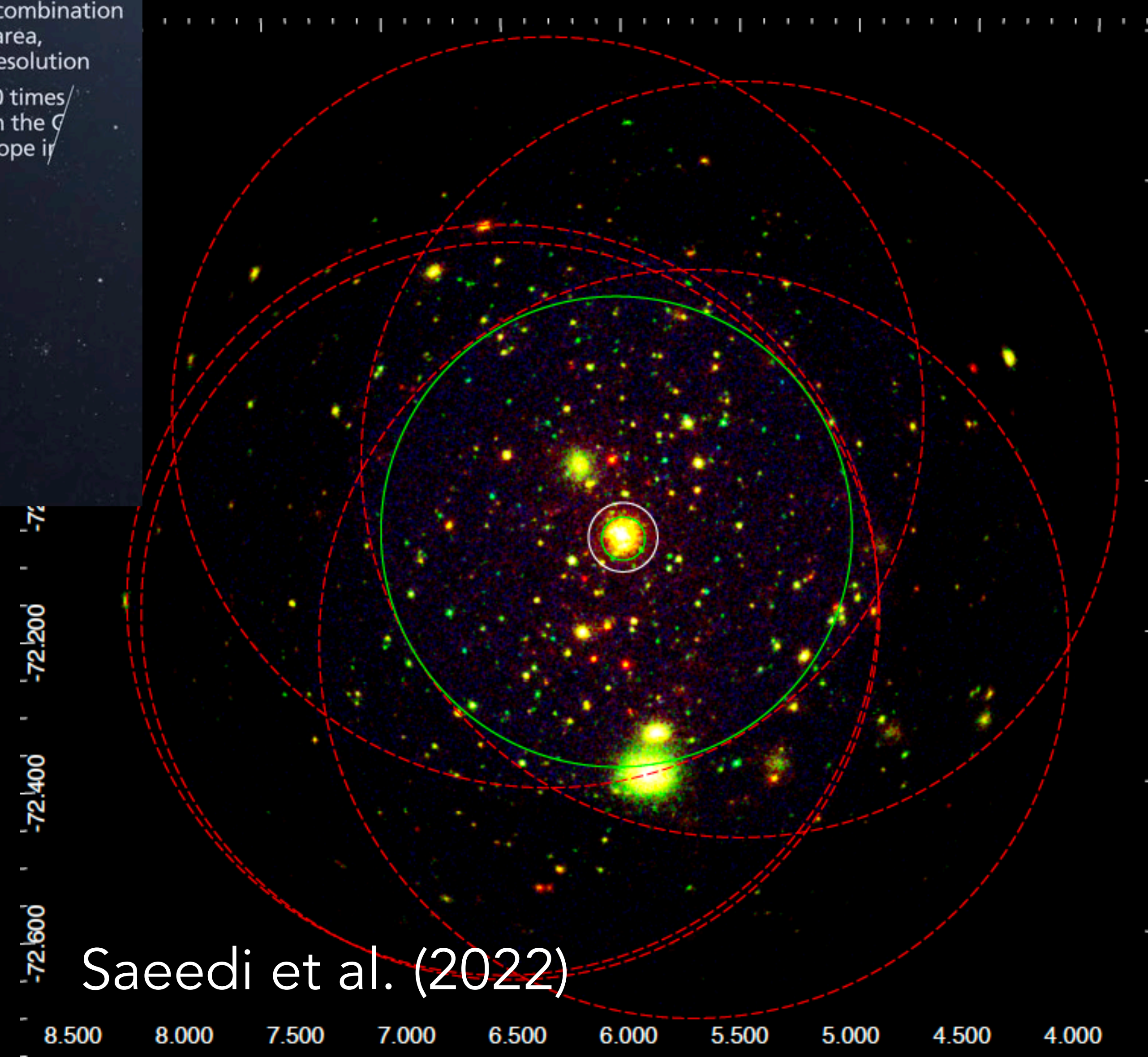

Saeedi et al. (2022)

TEV EXCESS AT GC

- Sub-threshold TeV halos possibly produce a significant fraction of TeV diffuse emission.
- Data from the 3HWC survey can be used for identifying possible TeV excess at the locations of GCs.
- Limiting flux @ few tens of TeV can provide a good constraint for the cutoff of IC component

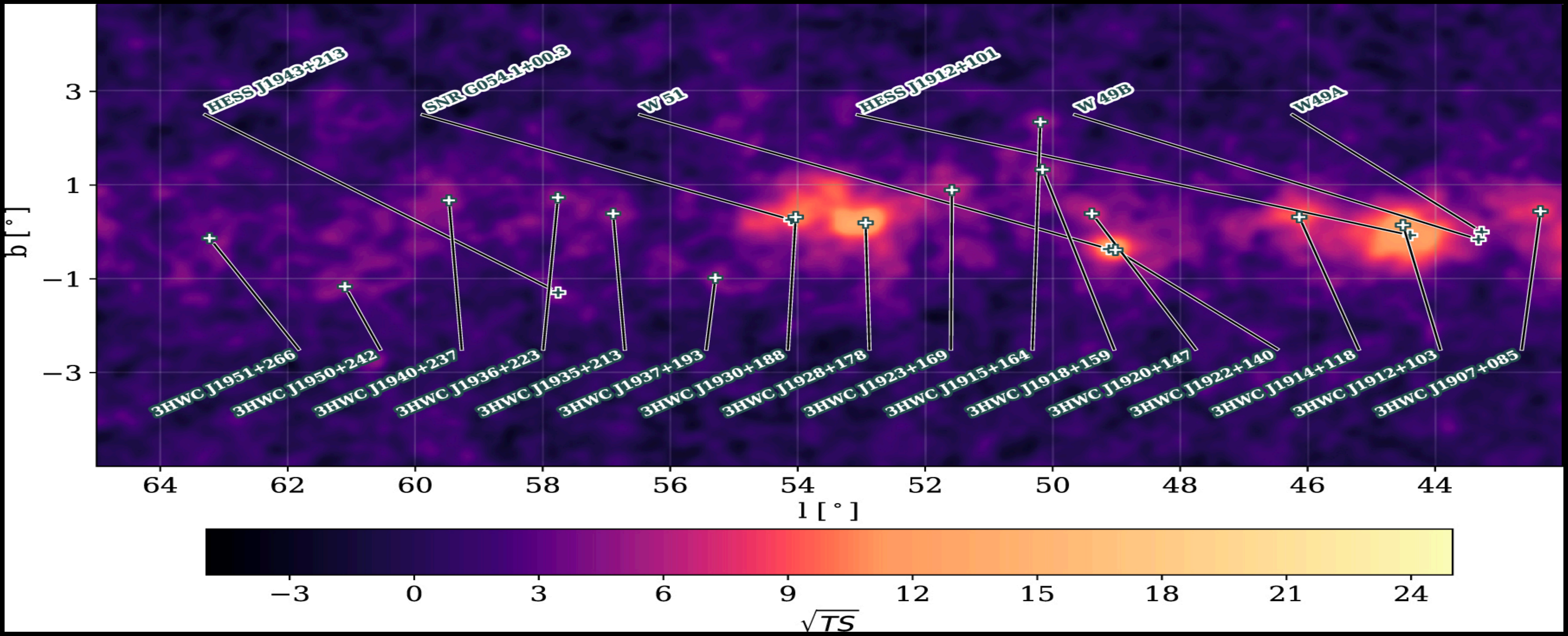

Albert et al. (2020)

TEV EXCESS AT GC

- Data from the 3HWC survey can be used for identifying possible TeV excess at the locations of GCs which are covered by the data.

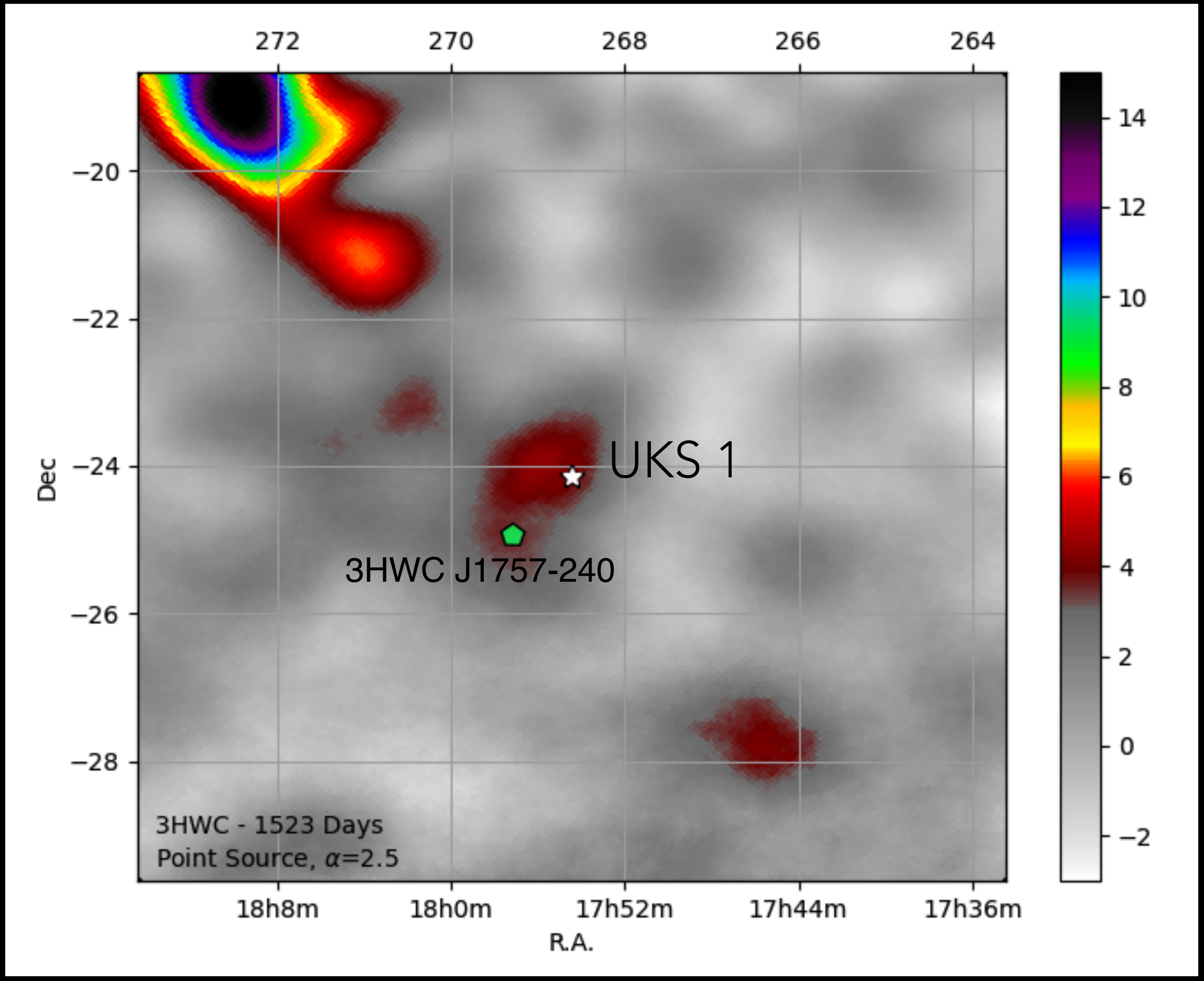

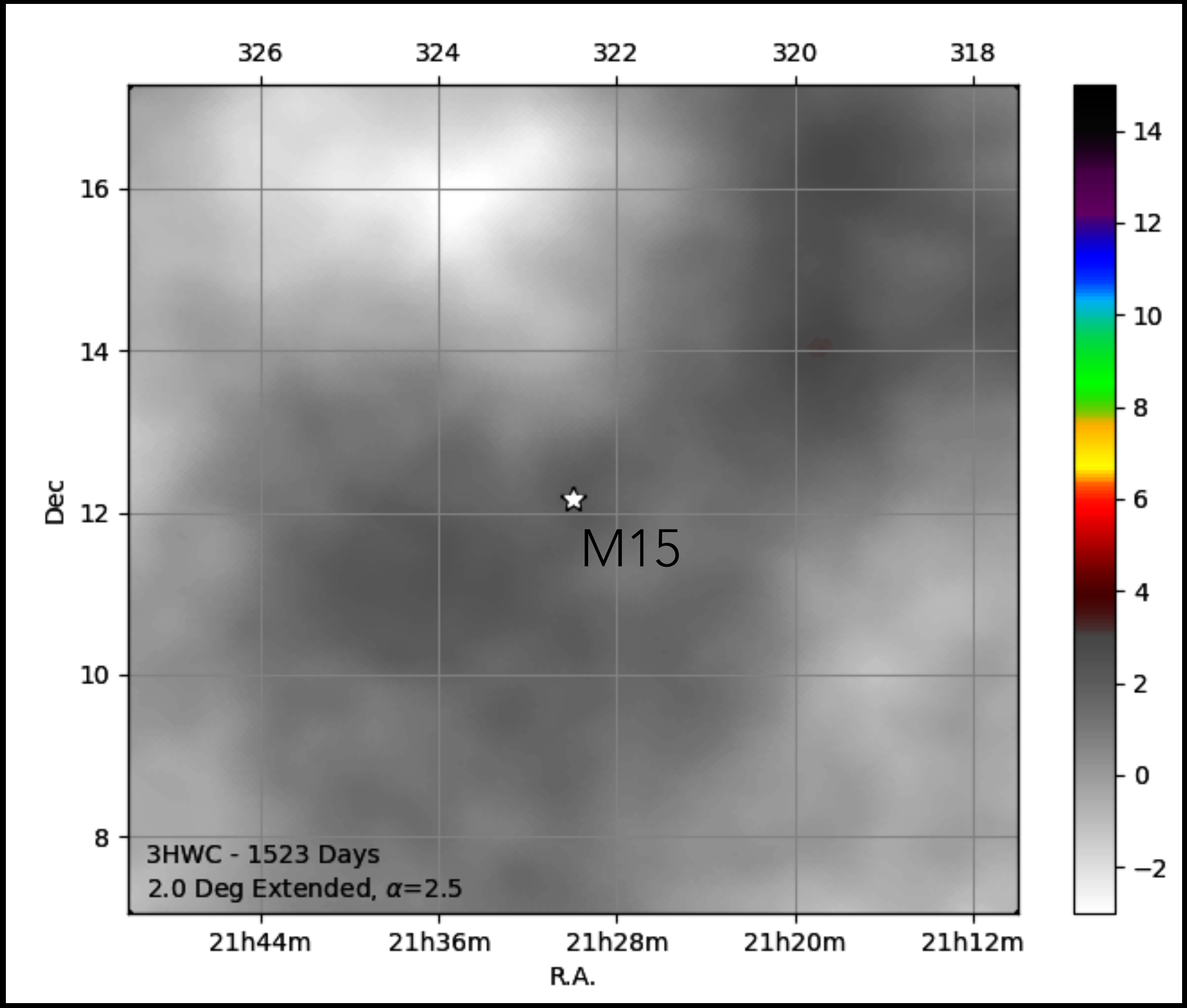

SUMMARY

- Dynamical interactions make GCs as efficient factories of MSPs.
- Frequent stellar encounters can make the physical properties (including high energy emission) of GC MSPs different from those in the GF.
- A significant fraction of GeV emission from GCs can be originated from ICS. It is possible the pulsar wind can also produce TeV-halo.
- We suggest a few "path-finder" analyses for identifying the GC TeV-halo candidates and provide constraint on a number of physical parameters (e.g. B-field, max. energy of particles)